UIN SUSKA RIAU

SURAT KEPUTUSAN REKTOR
UNIVERSITAS ISLAM NEGERI SULTAN SYARIF KASIM RIAU
Nomor : 0935 /R/2018

Tentang
PENETAPAN PENELITI PENELITIAN CLUSTER DASAR INTEGRASI KEILMUAN PADA LEMBAGA PENELITIAN DAN PENGABDIAN KEPADA MASYARAKAT UIN SULTAN SYARIF KASIM RIAU TAHUN ANGGARAN 2018

REKTOR UIN SULTAN SYARIF KASIM RIAU

Menimbang : a. bahwa dalam rangka untuk kelancaran kegiatan penelitian Cluster Dasar Integrasi Keilmuan pada Lembaga Penelitian dan Pengabdian Kepada Masyarakat UIN Sultan Syarif Kasim Riau Tahun 2018, maka dipandang perlu menunjuk Peneliti Penelitian Cluster Dasar Integrasi Keilmuan;
b. bahwa mereka yang namanya tercantum dalam Lampiran Surat Keputusan ini dianggap mampu dan cakap serta memenuhi syarat untuk melaksanakan tugas tersebut;
c. bahwa berdasarkan pertimbangan sebagaimana dimaksud dalam huruf a dan huruf b perlu menetapkan Surat Keputusan Rektor tentang Penunjukan sebagai Peneliti penelitian Cluster Dasar Integrasi Keilmuan pada Lembaga Penelitian dan Pengabdian Kepada Masyarakat UIN Sultan Syarif Kasim Riau Tahun 2018.

Mengingat :
1. Undang-Undang Nomor 20 Tahun 2003 tentang Sistem Pendidikan Nasional;
2. Undang-Undang Nomor 12 Tahun 2012 tentang Pendidikan Tinggi;
3. Undang-Undang Nomor 5 Tahun 2014 tentang Aparatur Sipil Negara;
4. Peraturan Pemerintah Nomor 4 Tahun 2014 tentang Penyelenggaraan Pendidikan Tinggi dan Pengelolaan Perguruan Tinggi;
5. Peraturan Menteri Agama RI Nomor 2 Tahun 2005 tentang Perubahan IAIN Susqa menjadi UIN Sultan Syarif Kasim Riau;
6. Peraturan Menteri Agama RI Nomor 9 Tahun 2013 jo Peraturan perubahannya No.74 Tahun 2013 tentang Organisasi dan Tata Kerja UIN Sultan Syarif Kasim Riau;
7. Peraturan Menteri Keuangan Republik Indonesia Nomor 49/PMK.02/2017 tentang Standar Biaya masukan Tahun Anggaran 2018.
8. Keputusan Menteri Keuangan RI Nomor 77/KMK.05/2009 tentang Penetapan UIN Sultan Syarif Kasim Riau pada Departemen Agama sebagai Instansi Pemerintah yang melaksanakan Pola Pengelolaan Keuangan Badan Layanan Umum;
9. Keputusanan Menteri Agama RI Nomor 23 Tahun 2014 tentang Statuta UIN Sultan Syarif KasimRiau;
10. Keputusanan Menteri Agama RI Nomor B.II/3/13847 tanggal 18 Juni 2014 tentang Pengangkatan Rektor UIN Sultan Syarif KasimRiau Periode 2014-2018;
11. Surat Pengesahan Daftar Isian Pelaksanaan Anggaran Badan Layanan Umum Petikan Tahun Anggaran 2017 Nomor SP DIPA-025.04.2.424157/2018, Tanggal 5 Desember 2017.

MEMUTUSKAN

Menetapkan : **SURAT KEPUTUSAN REKTOR TENTANG PENETAPAN PENELITI PENELITIAN CLUSTER DASAR INTEGRASI KEILMUAN PADA LEMBAGA PENELITIAN DAN PENGABDIAN KEPADA MASYARAKAT UIN SULTAN SYARIF KASIM RIAU TAHUN 2018.**

Pertama : Menetapkan Peneliti Penelitian Cluster Dasar Integrasi Keilmuan pada Lembaga Penelitian dan Pengabdian Kepada Masyarakat UIN Sultan Syarif Kasim Riau Tahun 2018 sebagaimana tercantum dalam lampiran yang merupakan bagian tidak terpisahkan dari Surat Keputusan ini.

Kedua.....

Kedua : Tugas Peneliti adalah:
1. Melaksanakan penelitian.
2. Mengikuti peraturan yang ditetapkan oleh LPPM.
3. Mengikuti seminar awal dan seminar akhir penelitian.
4. Mengumpulkan laporan hasil penelitian.
5. Mengumpulkan laporan keuangan penelitian.
6. Melaporkan hasilnya kepada Rektor.

Ketiga : Biaya Biaya pelaksanaan dibebankan kepada DIPA BLU UIN Sultan Syarif Kasim Riau tahun Anggaran 2018 Nomor SP DIPA-025.04.2.424157/2018, Tanggal 5 Desember 2017.:
Penelitian Cluster Dasar Integrasi Keilmuan Rp. 65.000.000,-per-judul

Keempat : Surat Keputusan ini mulai berlaku mulai bulan Mei s.d. Nopember 2018.

Kelima : Segala sesuatu akan diubah dan dibetulkan kembali sebagaimana mestinya, apabila terdapat kekeliruan dalam penetapan ini.

KUTIPAN Surat Keputusan ini disampaikan kepada yang bersangkutan untuk diketahui dan dilaksanakan.

Ditetapkan di : Pekanbaru
Pada Tanggal : 28 Mei 2018
Rektor,

Prof. Dr. H. Munzir Hitami, MA.
NIP. 19540422 198603 1002

Tembusan Keputusan ini disampaikan kepada :
1. Sekretaris Jenderal Kementerian Agama RI Jakarta;
2. Direktur Jenderal Pendidikan Islam Kementerian Agama RI Jakarta;
3. Inspektur Jenderal Pendidikan Islam Kementerian Agama RI Jakarta;
4. Direktur Pendidikan Tinggi Agama Islam Kementerian Agama RI Jakarta;
5. Wakil Rektor di Lingkungan UIN Sultan Syarif Kasim Riau;
6. Dekan Fakultas di Lingkungan UIN Sultan Syarif Kasim Riau;
7. Kepala Biro di lingkungan UIN Sultan Syarif Kasim Riau;
8. Kepala Kantor Pelayanan Perbendaharaan Negara Pekanbaru;
9. Kepala Bagian Keuangan dan Akuntansi UIN Sultan Syarif Kasim Riau;
10. Bendahara Pengeluaran DIPA BLU UIN Sultan Syarif Kasim Riau.

SURAT KEPUTUSAN REKTOR UIN
SULTAN SYARIF KASIM RIAU
Nomor : /R/2018
Tanggal : 2018

PENETAPAN PENELITI PENELITIAN CLUSTER DASAR INTEGRASI KEILMUAN PADA LEMBAGA PENELITIAN DAN PENGABDIAN KEPADA MASYARAKAT UIN SULTAN SYARIF KASIM RIAU TAHUN ANGGARAN 2018

No	JUDUL	PENELITI	RERATA NILAI	Anggota Peneliti
1	DAMPAK KEBAKARAN HUTAN DAN LAHAN TERHADAP KEBERLANGSUNGAN SOSIO-ECO-RELIGIO- CULTURE DI PROPINSI RIAU	HUSNI THAMRIN	315	Dr. Alpizar, M.Si (196406251992031004) Dr. Heri Sunandar, MCL.
2	IMPLEMENTASI TEXT MINING CLASSIFICATION SEBAGAI PEMODELAN DALAM PENYIMPULAN MUATAN TAFSIR BIL MA'TSUR DAN RA'YI PADA TAFSIR AL-MISBAH M. QURAISH SHIHAB BERBASIS MOBILE APPLICATION	Afrizal Nur	322,5	Mustakim () Sujai Sarifandi (197005031997031002)
3	KONSTRUKSI MODEL KURIKULUM INTEGRASI ILMU SOSIAL DAN ISLAM SERTA IMPLEMENTASINYA DALAM PEMBELAJARAN DI FAKULTAS TARBIYAH	Dr. Kadar, M.Ag	290	Dr. Alwizar, M.Ag (197004222003121002) Irawati, (520933)
4	MODEL KONSEPTUAL IMPLEMENTASI PENDIDIKAN KARAKTER TASAWUF DALAM PROSES PEMBELAJARAN.	Nurcahaya, S.Ag, M.Pd.I	450	RONI KURNIAWAN (8256) Madona Khairunnisa, M. Sy
5	PEMANFAATAN TUMBUHAN GULMA PERAIRAN SEBAGAI BAHAN ASAL PEMBUATAN ELEKTRODA SUPERKAPASITOR	Dr. Rika, S.Si, M.Sc	327,5	Susi Afriani, ST., MT (8327) Novi Gusnita, S.T., M.T. (197708032011012002)
6	PENANGKALAN RADIKALISME AGAMA DALAM PERSPEKTIF MAQASHID SYARI'AH (Studi di Markaz al-Maqashid li al-Dirasat wa al-Buhuts Maroko)	Dr. H. Mawardi Muhammad Saleh, Lc, MA	420	Fikri Mahmud (2821) Zulfahmi (197101011997031010)
7	PENGARUH FATWA MAJELIS ULAMA INDONESIA (MUI) NOMOR 4 TAHUN 2016 TENTANG IMUNISASI TERHADAP KEPUTUSAN ORANG TUA MELAKSANAKAN IMUNISASI DASAR ANAK DI PROVINSI RIAU	VIRNA MUSELIZA	292,5	Afrizal (196904192007011025) Devi Deswimar, S.Sos, M.SI
8	PENGARUH KEPUTUSAN INVESTASI, ENVIRONMENTAL CONCERN DAN KINERJA LINGKUNGAN TERHADAP PENGUNGKAPAN CORPORATE SOCIAL RESPONSIBILITY	Musfialdy, S.Sos, M.Si	415	Edison, S.Sos, M.I.Kom () Artis, S.Ag, M.I.Kom
9	PENGEMBANGAN BAHAN AJAR BAHASA INGGRIS CHARACTER-BASED INSTRUCTIONAL MATERIALS DENGAN MEDIA KARTU DI SMP NEGERI 4 PEKANBARU	Rizki Fiprinita,	340	Roswati, (197601222007102001) Idham Saputra, M. Ed

No	JUDUL	PENELITI	RERATA NILAI	Anggota Peneliti
10	PENGEMBANGAN VIRTUAL-MICROLAB KIMIA BERBASIS GREEN-CHEMISTRY TERINTEGRASI NILAI ISLAM UNTUK MENDUKUNG KETERAMPILAN BEREKSPERIMEN KIMIA DAN KARAKTER RELIGIUS SISWA	Yenni Kurniawati	410	Dra. Fitri Refelita, M.Si (196812311994032016) Dra. Afrida, M.Ag (196601131995032001)
11	PENGENDALIAN POSISI PADA SISTEM MAGNETIC LEVITATION BALL MENGGUNAKAN PENGENDALI OPTIMAL METODE LINEAR QUADRATIC REGULATOR (LQR)	Dian Mursyitah	385	Ahmad Faizal, ST, MT (198806302015031006) Sri Basriati
12	PENGUKURAN KINERJA RANTAI PASOK MENGGUNAKAN METODE SCOR MODEL DAN SOFTWARE PROCESS WIZARD (Studi Kasus Sertifikasi Produk Halal LPPOM MUI Riau)	Fitra Lestari Norhiza	467,5	Mawardi (197108091999031004) (198012162009121002) DEWI DINIATY (8309)
13	PERBANDINGAN MODEL HUJAN BERDASARKAN DATA HUJAN TAHUN MASEHI DAN TAHUN HIJRIAH	Rado Yendra	452,5	Ari Pani Desvina (198112252006042003) Muspika Hendri, S.Pd.I, MA (197709152007011015)
14	Possitive Psychotherapy Husnu-Dzhan : Model Pengembangan Psikoterapi Islam Dalam Menurunkan Derajat Stress Pada Penderita hipertensi	Mukhlis	290	Liliza Agustin (520407) Nurhayati, S. Pd. I, M. Pd
15	SISTEM PENENTUAN TINGKATAN TEMPO BACAAN AL QURAN MENGGUNAKAN METODE BACKPROPAGATION NEURAL NETWORK	Lestari Handayani, ST, M.Kom	322,5	Muhammad Fikry, ST, M.Sc (198010182007101002) Yusra, ST, MT (198401232015032001)
16	TINGKAT KETAATAN UMAT ISLAM TERHADAP FATWA MAJELIS ULAMA INDONESIA (MUI): STUDI KASUS DI PROVINSI NANGGRO ACEH DARUSSALAM, RIAU DAN DKI JAKARTA	Mohammad Abdi Almaktsur, M.A	435	Mardiana, M.A (197404101990032001) Rodi Wahyudi (8348) Syukran, S.H.I, M.Sy Zulikromi, Lc, M.A
17	TRANSFORMASI PESAN KONSERVASI SUMBER DAYA AIR DI KAWASAN SUAKA MARGASATWA BUKIT RIMBANG BALING KABUPATEN KAMPAR PROVINSI RIAU MELALUI KEARIFAN LOKAL BERBASIS NILAI-NILAI ISLAM	Dr. Nurdin, MA	410	Dewi Sukartik, M.Sc () Usman, M.I. Kom

Rektor,

Prof. Dr. H. Munzir Hitami, MA
NIP. 195404221983031002

LAPORAN PENELITIAN
Dasar Integrasi Keilmuan

PEMANFAATAN TUMBUHAN GULMA PERAIRAN SEBAGAI BAHAN ASAL PEMBUATAN ELEKTRODA SUPERKAPASITOR

Peneliti :
Dr. Rika, M.Sc
Susi Afriani, MT
Novi Gusnita, MT

LEMBAGA PENELITIAN DAN PENGABDIAN KEPADA MASYARAKAT (LPPM)
UIN SULTAN SYARIF KASIM RIAU 2018

LAPORAN AKHIR PENELITIAN

(Cluster Integrasi Keilmuan)

PEMANFAATAN TUMBUHAN GULMA PERAIRAN SEBAGAI BAHAN ASAL PEMBUATAN ELEKTRODA SUPERKAPASITOR

Oleh:

Dr. Rika, S.Si., M.Sc (Peneliti Utama)

Anggota Peneliti:
Susi Afriani, ST, MT
Novi Gusnita, MT
Marhama Jelita, M.Sc

Tim Penunjang
Dr. Erman Taer, M.Si (Universitas Riau)

LEMBAGA PENELITIAN DAN PENGABDIAN KEPADA MASYARAKAT
UNIVERSITAS ISLAM NEGERI SULTAN SYARIF KASIM RIAU

2018

DAFTAR ISI

BAB I

PENDAHULUAN

1.1 Latar Belakang Masalah

Indonesia merupakan negara kepulauan terbesar di dunia, dengan luas wilayah daratan sebesar 1.922.570 km² dan luas wilayah perairannya 3.257.483 km². Di wilayah daratan dijumpai ekosistem perairan umum berupa sungai, danau, waduk dan rawa dengan luas mencapai 540.000 km^2. Iklim tropis juga sangat berperan terhadap tumbuh suburnya berbagai jenis tumbuhan gulma air. Tumbuhan gulma air mampu tumbuh dan beradaptasi dengan cepat. Gulma air seperti rumput purun tikus (*Eleocharis dulcis*), eceng gondok (*Eichhornia Crassipes*) dan kiambang (*Pistia stratiotes L*) merupakan jenis gulma air yang memiliki sifat-sifat karakteristik laju perkembangan yang sangat cepat dengan sifat adaptasi yang tinggi di berbagai kondisi lingkungan. Keberadaan dari tumbuhan gulma air ini pada permukaan perairan dapat menimbulkan masalah ekosistim perairan seperti mengganggu transportasi air, mengakibatkan penurunan kualitas air, pendangkalan danau, sungai, waduk dan perairan lainnya, penyumbatan aliran air, penurunan debit air sungai serta mempercepat pendangkalan karena evaporasi. Selain merugikan karena dapat menimbulkan masalah pada lingkungan dan cepat menutupi permukaan air, tumbuhan gulma air ini dapat dimanfaatkan karena tumbuhan gulma ini mampu menyerap zat organik, anorganik, logam berat lain yang merupakan bahan pencemar di wilayah perairan serta dapat dijadikan sebagai bahan utama dalam pembuatan karbon aktif.

Purun tikus merupakan tumbuhan gulma yang tumbuh dan berkembang di lahan rawa pasang surut yang berlumpur, banyak ditemukan di daerah terbuka di lahan rawa yang tergenang air pada ketinggian 0−1.350 m di atas permukaan laut. Tumbuhan ini juga banyak ditemui di daerah persawahan yang tergenang air. Purun tikus dapat tumbuh dengan baik pada temperatur 30-35°C, dengan kelembapan tanah yang berkisar antara 98-100%. Tanah yang cocok untuk pertumbuhan purun tikus adalah tanah lempung atau humus dengan pH 6,9-7,3, tetapi purun tikus juga mampu tumbuh dengan baik pada tanah masam (Flach and Rumawas,1996). Eceng gondok merupakan gulma di air karena pertumbuhannya yang begitu cepat dan salah satu tanaman gulma

air yang banyak ditemukan di daerah tropis dan sub-tropis seperti di wilayah asia tenggara, pasifik, afrika dan beberapa daerah di amerika latin. Tumbuhan ini dapat beradaptasi dengan perubahan yang ekstrem dari ketinggian air, arus air, dan perubahan ketersediaan nutrien, pH, temperatur dan racun-racun dalam air (Gopal, 1987). Penyebaran dan pertumbuhan yang sangat cepat membuat eceng gondok menjadi sebuah masalah baru bagi daerah perairan yang dapat mengganggu keseimbangan ekosistem. Penggunaan tanaman gulma eceng gondok sebagai bahan utama dalam pembuatan karbon aktif yang telah dilakukan sebelumnya menunjukkan adanya potensi pemanfaatan yang menjanjikan seperti digunakan sebagai bahan penyerap logam berat dan sebagai piranti penyimpan energi seperti kapasitor dan Superkapasitor.

Pada penelitian ini akan ditinjau potensi pemanfaatan tumbuhan gulma di perairan sebagai elektroda karbon untuk superkapasitor. Tumbuhan gulma ini diolah melalui proses sederhana untuk dapat dijadikan sebagai karbon aktif tanpa perekat. Fokus penelitian ini adalah untuk mencari jalur pembuatan elektroda karbon tanpa perekat untuk aplikasi pada piranti superkapasitor dari tumbuhan gulma di perairan. Untuk mencapai energi dan daya yang tinggi, bahan elektroda superkapasitor harus memiliki luas permukaan spesifik (SSA) yang tinggi yang berfungsi untuk penyerapan ion, distribusi dan ukuran pori (PSD) dapat dioptimalkan untuk menghasilkan kombinasi energi dan daya spesifik yang diinginkan. SSA dan PSD sering dianggap sebagai dua faktor kunci yang mengendalikan energi dan daya dari sebuah superkapasitor.

1.2. Rumusan masalah

Peta jalan kegiatan dalam penelitian ini merujuk pada langkah-langkah untuk menghasilkan elektroda karbon dari tumbuhan gulma sebagai elektroda superkapasitor tanpa perekat. Objek yang akan dikaji dalam penelitian ini adalah menghasilkan elektroda karbon dengan proses aktivasi kimia dan fisika dari tumbuhan gulma untuk dapat digunakan sebagai elektroda aktif pada piranti penyimpan energi superkapasitor.

1.3 Signifikansi Penelitian

Pembuatan elektroda karbon secara umum dikerjakan menggunakan peralatan yang komplek dan biasanya menggunakan bahan asal dengan biaya produksi yang relatif tinggi. Penciptaan metode baru dalam jalur yang sederhana menggunakan bahan limbah biomasa merupakan alternatif yang perlu dilakukan untuk menekan biaya

produksi karbon. Langkah yang dilakukan adalah dengan mengunakan kombinasi waktu ball miling, penyaringan melalui seleksi bahan asal yang sesuai. Bahan asal alternatif yang dipilih sebagai prekursor dalam penelitian ini adalah rumput purun tikus, eceng gondok dan kiambang. Berbagai proses aktivasi dilakukan untuk kontrol ukuran pori guna menjamin kesesuai ukuran pori dari elektroda karbon yang dihasilkan dengan berbagai jenis elektrolit baik berbasis air. Diharapkan dapat diperoleh elektroda karbon teraktivasi dari tumbuhan gulma yang mempunyai nilai luas permukaan yang tinggi. Nilai luas permukaan akan diselidiki dengan uji BET. Disamping itu juga ditinjau strutur mikro dan morphologi elektroda karbon yang dihasilkan dengan analisa difraksi sinar-X (XRD), imbasan mikroskop elektron (SEM) dan energi dispersif sinar-X (EDX). Serangkaian kegiatan penyediaan dan karakterisasi elektroda karbon di akhiri dengan uji sifat kapasitif dengan cara merakit sel superkapasitor model koin. Uji sifat kapasitif akan dilakukan dengan beberapa metode seperti siklik voltammetri (CV) dan galvanostatik cas-discas.

1.4 Tujuan

Tujuan yang akan dicapai dalam penelitian ini adalah mengembangkan kemandirian dalam pembuatan elektroda karbon menggunakan tumbuhan gulma perairan sebagai bahan dasar pembutan elektroda superkapasitor tanpa perekat dengan biaya rendah. Adapun tujuan secara khusus adalah sebagai berikut :

a. Menghasilkan elektroda karbon superkapasitor yang bersifat swa-merekat menggunakan bahan-bahan dari tumbuhan gulma perairan (purun tikus, eceng gondok, kiambang)
b. Menyelidiki sifat morphologi permukaan, luas permukan, struktur kristal, kandungan elemen bahan elektroda karbon mengunakan beberapa metoda seperti imbasan mikroskop elektron, serapan gas N_2, difraksi sinar-X, dan energi dispersive sinar-X.
c. Menyelidiki sifat elektrokimia elektroda karbon dengan membangun sel superkapasitor melalui uji siklik voltammetri dan cas-discas menggunakan elektrolit berbasis air.
d. Menganalisa lebih jauh kesesuaian karbon aktif dari tumbuhan gulma perairan sebagai elektroda superkapasitor tanpa perekat/monolit.

1.5 Penerapan Hasil Kegiatan

Apabila elektroda karbon berbasis bahan biomassa berasal dari tumbuhan gulma perairan dapat diproduksi sebagai elektroda superkapasitor, maka sebagai keunggulan penelitian ini adalah ketersediaan bahan elektroda dengan biaya murah serta dampak sampingnya adalah pengendalian tumbuhan gulma perairan dapat dilakukan sehingga kelestarian lingkungan perairan dapat juga dipertahankan.

Secara khusus sampai akhir masa penelitian yang direncanakan diharapkan pemanfaatan tumbuhan gulma perairan dapat memperkaya ketersediaan bahan asal dalam pembuatan elektroda karbon superkapasitor. Dengan semakin meningkatnya keberagaman bahan asal pembuatan elektroda tentu dapat digunakan untuk menekan biaya produksi pembuatan piranti superkapasitor. Keberhasilan pengembangan elektroda superkapasitor berbasis bahan biomassa dapat dijadikan tonggak untuk meningkatkan pengunaan superkapasitor pada berbagai bidang aplikasi seperti mobil hibrida, kereta api, peralatan elektronik dan lain sebagainya. Lebih jauh lagi, potensi alam dan lingkungan yang dimiliki oleh Indonesia akan menjadi unik dan kompetitif dalam dunia internasional apabila mampu membuka terobosan teknologi. Untuk mencapai hal tersebut, pendekatan lintas bidang menjadi penting dalam penelitian ini, terutama untuk mengkombinasikan ilmu dan teknologi dengan keunggulan potensi alam agar mempunyai nilai tambah baik secara teknologi nano dalam skala industri.

BAB II

TINJAUAN KEPUSTAKAAN

2.1. Pengenalan

Superkapasitor atau ultrakapasitor [3] adalah istilah yang digunakan untuk piranti penyimpan energi listrik yang mempunyai nilai kapasitan mencapai ribuan farad. superkapasitor menjadi piranti penyimpan energi listrik yang baik untuk penyimpanan energi. Komemersial produk superkapasitor mempunyai spesifik energi dibawah 10 Wh kg^{-1}, lebih rendah jika dibandingkan dengan batterai litium ion batterai dapat mencapai 150 Wh kg^{-1}. Superkapasitor mempunyai spesifik daya yang lebih tinggi dari betterai. Sisi positif lain adalah siklus hidup yang lebih tinggi, dapat dioperasikan pada jangkauan temperatur yang lebih besar dan cas serta dis cas yang cepat.

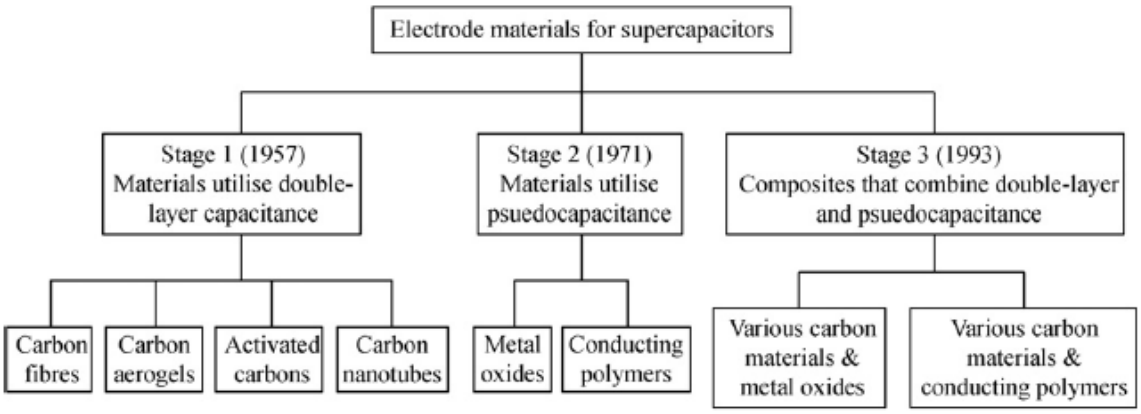

Gambar 1. Perkembangan penyelidikan bahan elektroda superkapasitor.

Penyelidikan pada supercapasitor dapat dibagi dalam dua kelompok berdasarkarkan pada cara penyimpanan energi yang disebut: 1) superkapasitor redox dan 2) kapasitor elektrokimia dua lapisan. Superkapasitor redox (juga dikenal dengan istilah *pseudocapacitor*), dimana sebuah tipe transfer muatan refersibel Faradaic yang menghasilkan kapasitan, yang bukan elektrostatik murni (sehingga diberi awalan ‘pseudo’ yang membedakan dari kapasitan electric statik). Sedangkan, penyimpanan tenaga pada kapasitor elektrokimia dua lapisan (KEDL) hampir menyerupai kapasitor tradisional yaitu melalui pemisahan muatan. Superkapasitor dapat menyimpan lebih banyak energi per unit masa atau volume dari pada kapasitor konvensional karena: 1)

pemisahan muatan terjadi pada jarak yang sangat kecil pada KEDL yang terjadi pada perbatasan elektoda dan elektrolit [4] 2) jumlah muatan yang dapat tersimpat dapat ditingkatkan dengan luas permukaan yang tinggi. Mekanismen penyimpanan energi berlangsung secara cepat karena melibatkan perpindahan ion dari dan keluar permukaan elektroda. Pembagian lengkap tentang jenis bahan elektroda ditampilkan pada Gambar 1. Superkapasitor jenis KEDL adalah kategori supercapasitor yang sangat maju dikembangkan. Karbon dalam berbagai bentuk, secara intensif terus di kaji dan digunakan secara meluas sebagai materila elektrod pada KEDL yang pengembangan di fokuskan pada pencapaian luas permukaan yang lebih tinggi dengan berbagai bahan asal yang lebih murah, limbah perkotaan merupakan bahan asal yang potensial dijadikan bahan asal elektroda superkapasitor dengan harga yang relatif murah.

2.2. Struktur KEDL

Struktur superkapasitor terdiri dari dua buah elektroda yang terendam dalam elektrolit, dengan sebuah pemisah ion-permeabel yang terletak diantara kedua elektroda, seperti yang ditunjukkan pada Gambar 2. Dalam piranti seperti itu, masing-masing antar muka elektroda elektrolit mewakili sebuah kapasitor sehingga sebuah sell lengkap dapat dipandang sebagai dua kapasitor tesusun secara seri. Untuk kapasitor simetris (elektroda yang sama), kapasitan sell, ditunjukkan sebagai :

$$\frac{1}{C_{Cell}} = \frac{1}{C_1} + \frac{1}{C_2} \quad (1)$$

Dimana C_1 dan C_2 mewakili kapasitan untuk elektrod pertama dan kedua [5]. Kapasitan dwi-lapisan , C_{dl}, pada masing-masing antara muka elektrod ditunjukkan dengan rumusan

$$C_{dl} = \frac{\varepsilon A}{4\pi t} \quad (2)$$

Dimana ε adalah konstanta dielektrik dari daerah dwi-lapisan, A adalah luas permukaan dari elektroda dan t adalah tebal dari dwi-lapisan elektrik. Pada kapasitor dwi-lapisan, merupakan kombinasi dari luas permukaan yang tinggi (biasanya > 1500 $m^2 g^{-1}$) dengan pemisahan muatan yang sangat kecil (Angstroms) yang dapat menghasilkan kapasitan yang tinggi [6]. Energi (E) dan daya (P_{max}) dari superkapasitor dapat ditentukan berdasarkan

$$E = \frac{1}{2} CV^2 \quad (3)$$

$$P_{max} = \frac{V^2}{4R} \quad (4)$$

Dimana C adalah kapasitan dc dalam Farads, V adalah tegangan dan R adalah eguivalen tahanan series (ESR) dalam ohm [6].

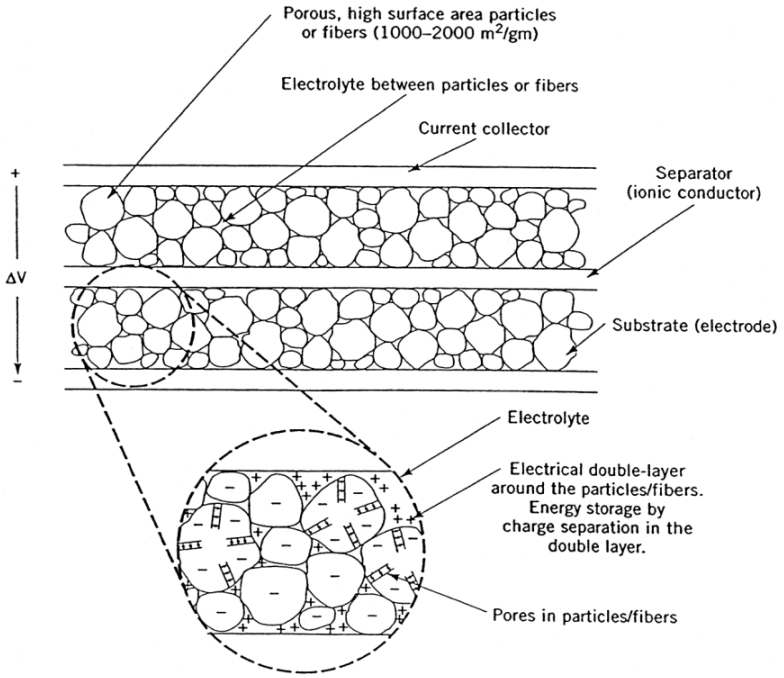

Gambar 2. Struktur superkapasitor

BAB III
METODOLOGI PENELITIAN

3.1 Prosedur Penelitian

Adapun metodologi penelitian ini akan melalui tahapan-tahapan seperti yang digambarkan dalam diagram alir berikut ini pada Gambar 3. Dimana sampel tumbuhan gulma perairan yang diteliti untuk dijadikan elektoda piranti superkapasitor adalah Rumput purun Tikus dan Tanaman Eceng gondok. Sampel tumbuhan pertama sekali mengalami penjemuran dan pengeringan,dipotong-potong dan di prakarbonisasi. Setelah itu dihancurkan sampai menjadi serbuk dengan ukuran partikel yang seragam dengan melalui proses pengayakan. Selanjutnya beberapa proses aktivasi kimia dan fisika dan sampai dihasilkannya pellet karbon setelah melalui proses pencetakan. Akhir sekali adalah proses perakitan sel superkapasitor dan proses pengujian sifat elektrokimia menggunakan cyclic voltrammetry (CV) dan Galvanostatik cas-discharge.

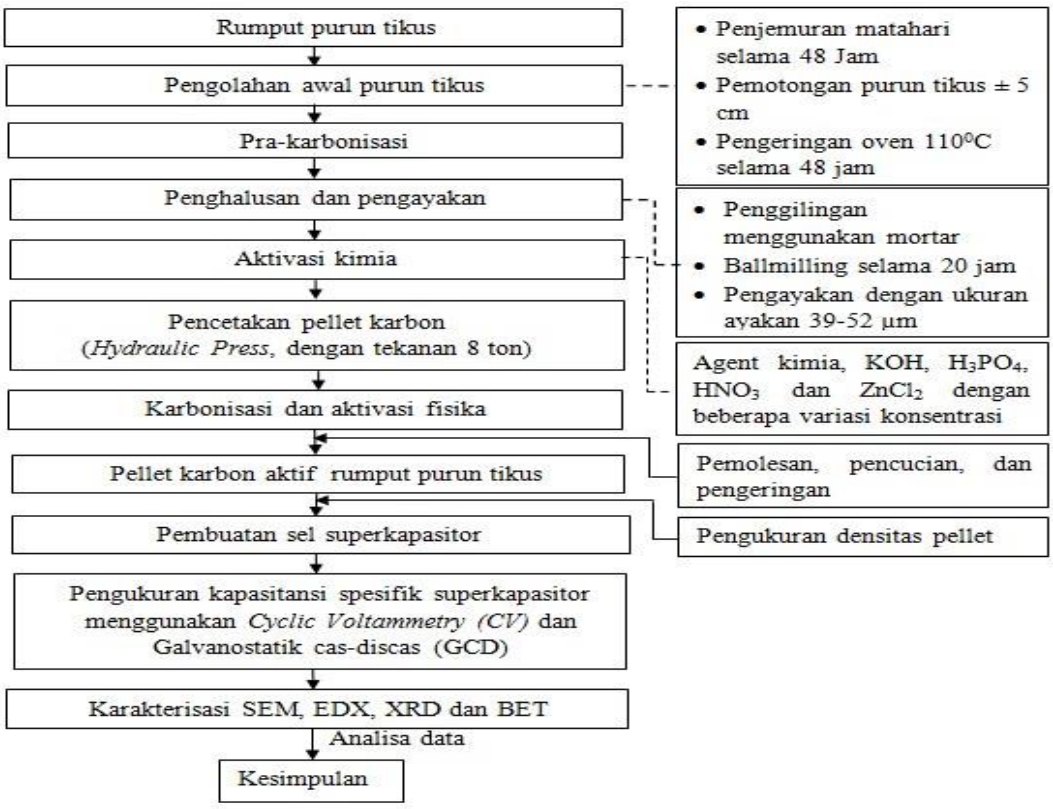

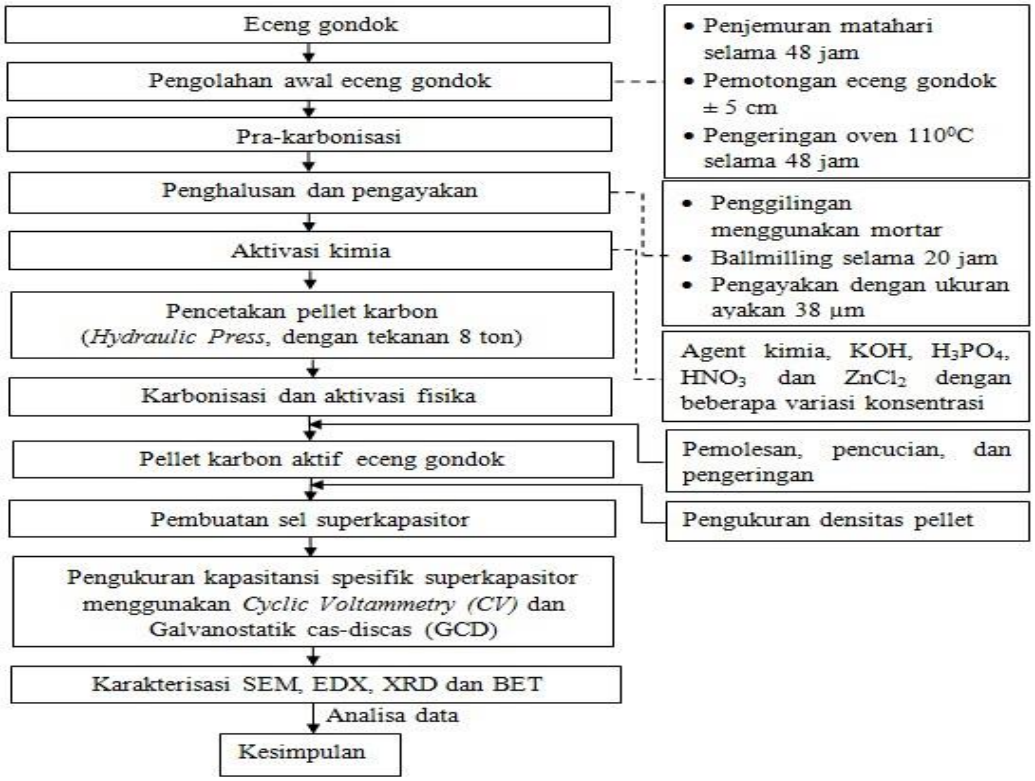

Gambar 3. Diagram alir penelitian dan luaran kegiatan penelitian

Untuk pengujian karakterisasi bahan elektroda dari tanaman gulma perairan ini, sampel akan diuji luas permukaannya dengan Scanning Electron Micrograph (SEM) mikrograf dan Energy Dispersive X-Ray (EDX) untuk mendeteksi kandungan carbon dan unsur-unsur yang dibawanya. Dan serangkaian uji XRD dan BET untuk mengobservasi sifat kekristalan dan ukuran porositas elektroda.

3.2 Uraian Lengkap Kegiatan Penelitian

Metode penelitian yang akan direncanakan selama enam bulan pelaksanaan efektif ini dibagi menjadi tiga bagian. Fokus penelitian setiap fasenya ditujukan pada pemilihan bahan dasar yang digunakan. Bahan dasar dalam pembuatan elektroda superkapasitor pada penelitian fase pertama difokuskan pada rumput purun tikus, fase kedua pemanfaatan eceng gondok. Setiap fase kegiatan dalam proses penelitian diawali dengan persiapan bahan dasar hingga pengujian sifat fisika dan sifat elektrokimia dan disertai dengan fabrikasi sel superkapasitor. Secara lengkap diagram alir penelitian untuk setiap fase di tampilkan pada Gambar dibawah ini. Ketua peneliti bertanggungjawab mengontrol pelaksanaan kegiatan secara keseluruhan khususnya

dalam pembuatan elektroda karbon untuk superkapasitor dari tanaman gulma air, serta membuat laporan hasil kegiatan. Anggota peneliti satu (1) bertanggungjawab dalam merancang dan mengontrol pelaksanaan penelitian. Peneliti satu dan dua juga sama-sama bertanggung jawab dalam merevisi draf dan submisiion artikel ilmiah. Sementara anggota penunjang memberikan fasilitas pemakaian Laboratorium dan pengukuran serta ikut andil dalam diskusi-diskusi peningkatan kualitas penelitian dan produk yang dihasilkan. Elektrolit yang digunakan dalam sel superkapasitor adalah asam sulfat dan kemudian ditambah bahan aditif sehingga pergerakan ion lebih efektif dan sifat kapasitan dapat ditingkatkan. Pelaksanaan kegiatan dilaboratorium Teknik Industri Uin Suska Riau dan di Laboratorium Fisika material Universitas Riau, Pekanbaru.

3.3 Jadwal Kegiatan

Item	Kegiatan	**Bulan ke-**					
		1	**2**	**3**	**4**	**5**	**6**
1	Merancang pelaksanaan eksperimen						
2	Pengumpulan Bahan mentah						
3	Pembelian bahan kimia						
4	Pre-carbonization						
5	Aktivasi kimia						
6	Karbonisasi						
7	Aktivasi Fisika						
8	Polishing and washing						
9	Karakterisasi Karbon aktif						
*	*High surface area of ACM*						
10	Fabrikasi Sel supercapasitor						
11	Karakterisasi Sel supercapasitor						
*	*High energy and power of EC based on ACM*						
12	Laporan dan persiapan draft untuk publikasi internasional						

***milestone**

3.4 Road Map Penelitian

Road map penelitian dapat dirici sebagai berikut. Tahun 2013-2014 capaian penelitian adalah pembuatan elektroda superkapasitor komposit dari bahan karbon dan logam oksida, masih bahagian road map bersama dengan rekan sejawat dari Universitas Riau. Tahun 2015-2017 capaian adalah dihasilkannya nano karbon fiber dari bahan biomassa untuk elektroda kapasitor, bersama dengan rekan sejawat dari Universitas Riau. Tahun 2018-2019 capaiannya adalah dihasilkannya sel superkapasitor berbasis elektroda karbon nano fiber dengan elektrolit diadditif secara kimia, road map sudah diarahkan menjadi road map pribadi. Tahun 2020-2022 adalah dihasilkannya superkapasitor berbasil elektrolit organik dengan bantuan bahan biomassa seperti pati sagu, kentang untuk superkapasitor tahan kering. 2023-2025 ditargetkan dapat dihasilkannya sel superkapasitor unggul berbasis nano karbon dari bahan biomassa dengan elektrolit berbasis bahan organik yang anti kering sehingga ini akan menjadi batu loncatan pertama untuk target kerja pengembangan keilmuan selama 12 tahun. Target berikutnya akan dijabarkan lagi menjadi beberapa target kecil dan target besar untuk beberapa tahun selanjutnya guna menghasilkan batu loncatan kedua. Demikianlah seterusnya pengembangan keilmuan yang dilakukan berdasarkan tetapan target sehingga dapat dicapai tepat sasaran dan terarah. Dalam bentuk diagram road map penelitian ditampilkan dalam Gambar 4 dibawah.

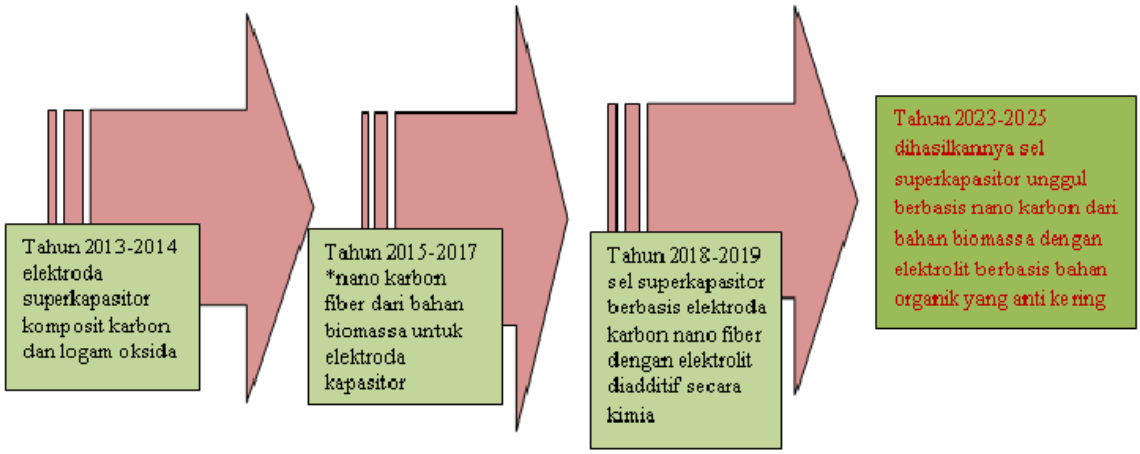

Gambar 4. Road Map penelitian hingga tahun 2025.

BAB IV
HASIL DAN PEMBAHASAN

4.1 Elektroda Karbon dari Eceng Gondok

4.1.1 Analisa Sifat Termal

Sifat termal karbon aktif dari eceng gondok dianalisis dengan menggunakan Thermogravimetric (TG) dan Diferensial Termografi Termal (DTG). Parameter yang diteliti adalah perubahan massa sampel terhadap perubahan suhu. DTG digunakan untuk mengukur laju perubahan massa sampel terhadap kenaikan suhu. Kedua analisis ini dilakukan pada kisaran suhu 30-600 ° C pada laju pemanasan 10 °C min^{-1} dalam lingkungan gas N_2. Massa sampel untuk analisis termal adalah 7,199 mg. Data sifat termal untuk sampel eceng gondok sebelum karbonisasi ditunjukkan pada Gambar 5.

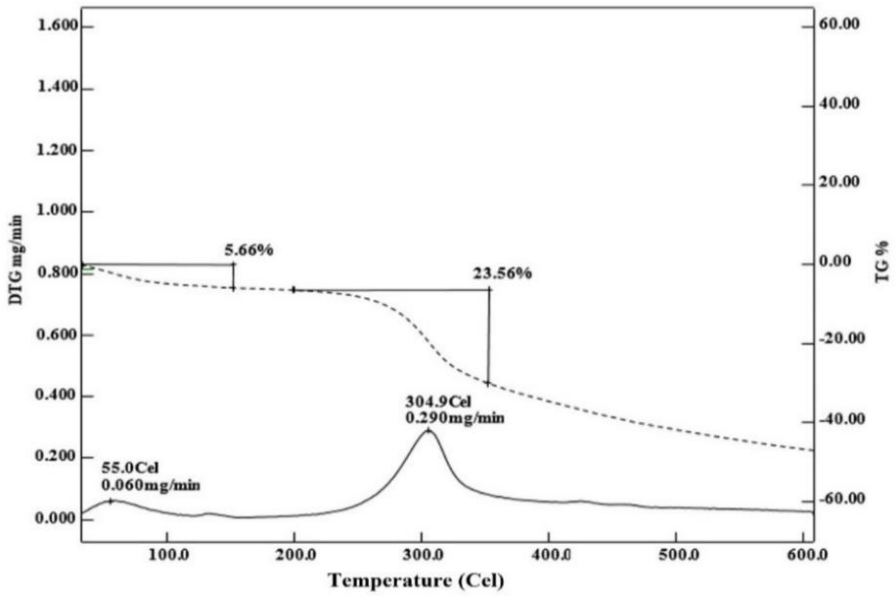

Gambar 5. The TG, dan kurva profil DTG untuk sampel enceng gondok

Gambar 5 menunjukkan profil perubahan massa sampel dalam persen (%) terhadap suhu (C). Kurva TG pada Gambar 1 diwakili oleh garis putus-putus. Data TG menunjukkan pola pengurangan massa sampel ketika suhu dinaikkan. Penurunan massa yang signifikan terjadi pada kisaran suhu 30-151 °C, 210-353 °C dan kemudian massa sampel menurun secara bertahap dari suhu 353-600 °C. Pengurangan massa pertama pada rentang suhu pertama 30-151 °C setinggi 5,66% dipengaruhi oleh pelepasan kadar air (Luo *et al*. 2011; Madrid *et al*. 2013;Gao *et al*. 2013). Yang kedua pada kisaran temperatur 210-353 °C sebesar 23,56% dipengaruhi oleh dekomposisi simultan selulosa

dan hemiselulosa (Yao *et al.* 2008), sedangkan pada tahap ketiga pengurangan massa sampel terjadi karena dekomposisi lignin (Fisher *et al.* 2002; Harun *et al.* 2011).

Kurva DTG ditunjukkan oleh garis padat pada Gambar 5, bentuk kurva ditandai dengan adanya dua puncak pada suhu 55 °C dan 304,9 °C, masing-masing. Puncak ini menunjukkan laju reduksi massa optimum terhadap suhu. Puncak pertama menunjukkan laju degradasi massa optimum pada kisaran suhu 30-151 °C oleh 0,060 mg min^{-1}, sedangkan pada puncak kedua menunjukkan laju degradasi massa optimum yang dialami oleh sampel adalah 0,290 mg min^{-1} dan terjadi pada kisaran suhu 210-353 °C. Temperatur 304,9 °C ini menunjukkan laju degradasi massa optimum yang merupakan dekomposisi maksimum dari elemen dasar sampel untuk meningkatkan unsur karbon. Suhu ini kemudian dipilih sebagai suhu resistan dalam proses karbonisasi sampel untuk memastikan tingkat kemurnian karbon yang lebih tinggi.

4.1.2 Massa, diameter, ketebalan dan kerapatan elektroda

Hasil pengukuran massa, diameter, ketebalan, dan densitas elektroda sebelum dan sesudah aktivasi karbonisasi, dan setelah proses pemolesan ditunjukkan pada Tabel 1. Massa, diameter, ketebalan, dan densitas elektroda sebelum aktivasi karbonisasi Prosesnya hampir sama, hasil ini masuk akal karena perlakuan sampel yang sama sementara perbedaan hasil adalah karena serbuk pra-karbon yang terbuang selama proses pencetakan pada tekanan kompresi. Massa, diameter, ketebalan, dan kepadatan elektroda CMWH setelah proses aktivasi karbonisasi mengalami penurunan karena pelepasan bahan non-karbon selama proses aktivasi karbonisasi (Farma *et al. et al.* 2013). Massa elektroda CMWH setelah proses pemolesan menunjukkan perbedaan, hal ini disebabkan oleh perbedaan ketebalan elektroda, ketebalan elektroda yang lebih besar akan menghasilkan massa elektroda yang lebih tinggi. Sedangkan diameter elektroda setelah proses pemolesan juga memiliki perbedaan, hal ini disebabkan oleh erosi elektroda selama pemolesan. Perbedaan kerapatan elektroda setelah pemolesan karena perbedaan ketebalan untuk setiap sampel. Kepadatan tertinggi ditemukan oleh sampel CMWH3 dengan ketebalan elektroda 0,30 mm yaitu 0,70 gcm^{-3}, sedangkan nilai densitas terkecil adalah CMWH1 sampel dengan ketebalan 0,26 mm yaitu 0,65 g cm^{-3}. Hasil ini dipengaruhi oleh perubahan massa dan diameter karena proses pemolesan.

Tabel 1. Massa (g), diameter (mm), ketebalan (mm), dan densitas (g cm^{-3})

Kode sampel	Sebelum Karbonisasi-aktivasi				Setelah Karbonisasi-aktivasi				Setelah pemolesan			
	m	d	t	ρ	m	d	t	ρ	M	d	t	ρ
CMWH1	0.582	19.72	0.235	0.81	0.192	13.58	0.162	0.82	0.022	12.90	0.26	0.65
CMWH2	0.59	19.95	0.243	0.78	0.195	13.85	0.161	0.80	0.0235	12.68	0.28	0.66
CMWH3	0.573	19.78	0.234	0.80	0.213	14.29	0.168	0.79	0.028	13.01	0.30	0.70

4.1.3 Analisa Serapan gas N_2

Gambar 6a menunjukkan data isotermis adsorpsi-desorpsi gas N pada sampel elektroda karbon, data ini menunjukkan hubungan antara volume adsorpsi-desorpsi dengan tekanan relatif (P/P_0). Model adsorpsi-desorpsi gas N_2 yang ditunjukkan pada Gambar 6a adalah tipe IV menurut klasifikasi IUPAC meskipun ada sedikit perbedaan dalam kondisi tekanan yang relatif besar. Penegasan tipe IV ditunjukkan oleh peningkatan volume penyerapan pada tekanan relatif 0,4.

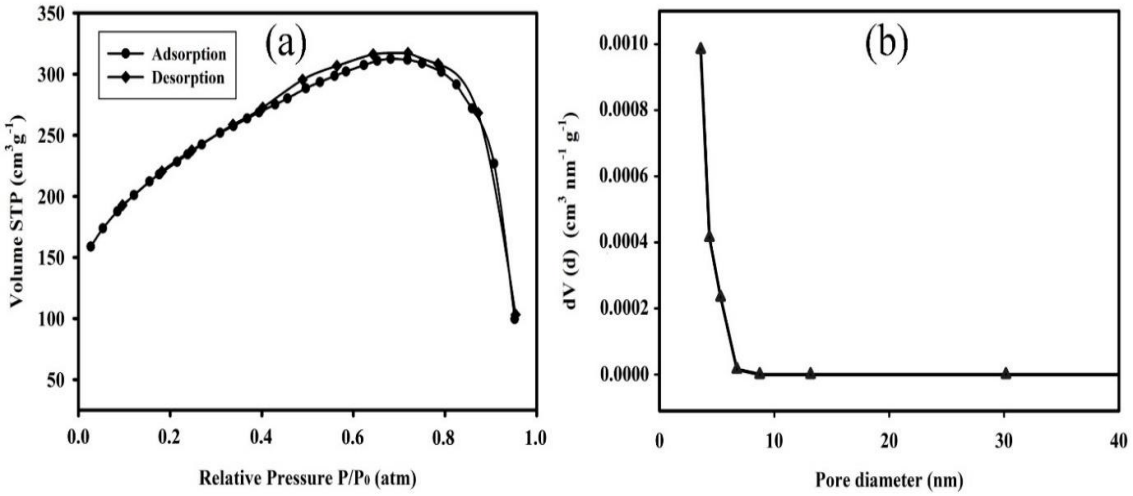

Gambar 6. (a) adsorpsi-desorpsi isotermal gas N_2 dan (b) distribusi ukuran pori

Gambar 6b menunjukkan hubungan antara dV/dr (d) ke diameter pori sampel menggunakan metode BJH. Metode BJH digunakan untuk melihat distribusi pori dari kisaran 3,5 hingga 40 nm. Dapat dilihat bahwa penurunan volume pori terjadi pada kisaran diameter pori 3,5-7,0 nm dan menunjukkan volume pori maksimum pada diameter 3,5 nm dari 0,001 $cm^3nm^{-1}g^{-1}$. Volume penyerapan maksimum menunjukkan bahwa diameter pori sampel dominan berada dalam kisaran mesopori. Penegasan data adsorpsi-desorpsi tipe IV diperkuat dengan rata-rata diameter pori BJH 3,5911 nm, yang menunjukkan diameter pori rata-rata sampel dalam kelompok mesopori yang sesuai dengan karakteristik tipe IV (Senthilkumar *et al.* 2013). Senthilkumar dkk. 2013 dengan

bahan yang sama juga memperoleh diameter pori dalam kisaran mesopori (Senthilkumar *et al.* 2013).

Data luas permukaan spesifik (S_{BET}), luas permukaan BJH, volume BJH, dan diameter ditunjukkan pada Tabel 2. Zhang et al, 2012 dan Kurniawan dkk, 2015 juga mempelajari materi yang sama yang diperoleh luas permukaan spesifik (SBET) sebesar 579,94 $m^2 g^{-1}$ (Zhang *et al.* 2012) dan 761 $m^2 g^{-1}$ (Kurniawan *et al.* 2015).

Table 2. Hasil pengukuran serapan gas N_2 dari sampel eceng gondok

Sample	S_{BET} ($m^2 g^{-1}$)	S_{BJH} ($m^2 g^{-1}$)	V_{BJH} ($cm^3 g^{-1}$)	D_{BJH} (Å)
CMWH	776.213	130.548	0.133	35.911

4.1.4 Analisa Morfologi Permukaan

Gambar 7a dan 7b menunjukkan sampel SEM mikrograf CMWH pada pembesaran 5000x dan 40000x. Gambar 3a dengan menunjukkan morfologi permukaan CMWH yang berbentuk seperti gumpalan dan didominasi oleh warna hitam yang diasosiasikan dengan partikel karbon dan juga terlihat partikel yang berwarna putih halus menunjukkan unsur-unsur lain selain karbon. Pada pembesaran ini, tidak ada makropori pada permukaan sampel CMWH. Sedangkan Gambar 7b adalah pembesaran di daerah ditandai dengan warna merah pada Gambar 7a. Partikel halus ini memiliki bentuk yang cenderung teratur dengan bentuk oval yang didominasi oleh panjang 0,44 μm dan lebar 0,38 μm.

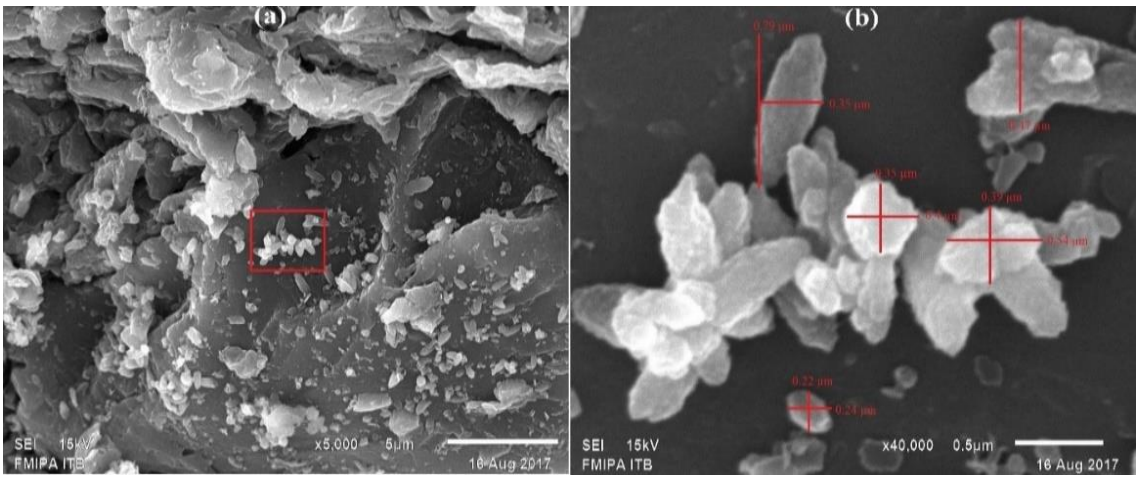

Gambar 7. Mikrograf SEM dari sampel CMWH (a) CMWH pada perbesaran 5000x (b) CMWH pada perbesaran 40000x

4.1.5 Analisa Kandungan Unsur

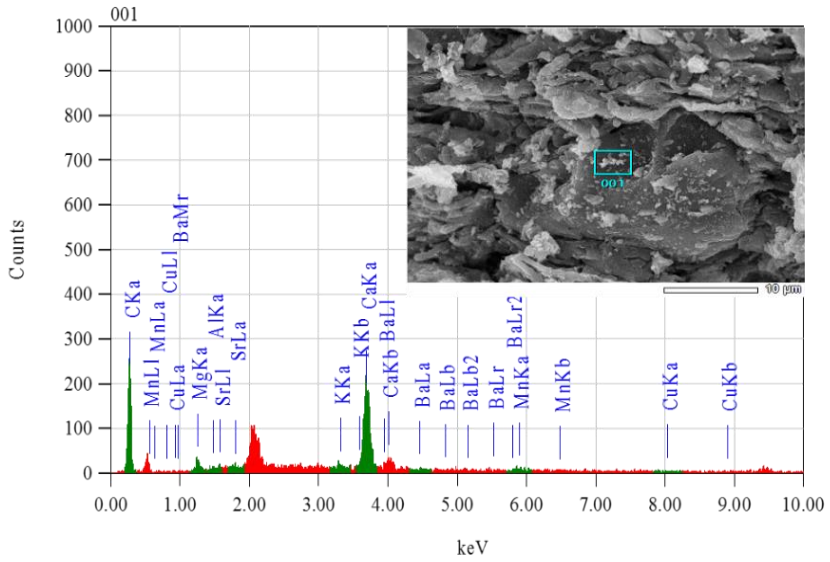

Gambar 8. Hasil pengujian menggunakan Energi dispersif sinar-X sampel eceng gondok

Hasil uji EDX dari sampel ditunjukkan pada Gambar 8 yang dipilih di area 15 µm2 yang ditunjukkan oleh kotak hijau dalam gambar SEM yang disisipkan di sisi kanan atas. Data EDX menunjukkan unsur-unsur yang terkandung dalam sampel CMWH yaitu karbon (C), magnesium (Mg), kalium (K), kalsium (Ca), mangan (Mn), tembaga (Cu), strontium (Sr) dan barium (Ba). Kandungan unsur-unsur penyusun sampel didominasi oleh karbon dan kalsium pada 0,277 keV dan 3,690 keV yang ditunjukkan oleh jumlah tertinggi, masing-masing. Persentase massa dan atom adalah 69,74%, 88,55%, untuk karbon dan 24,44%, 9,30% untuk kalsium, masing-masing. Unsur-unsur lain seperti Magnesium, kalium, mangan, tembaga, strontium, dan barium dengan energi 1,253 keV, 3,312 keV, 5,894 keV, 8,040 keV, 1,806 keV dan 4,464 keV, masing-masing. Studi lain dengan bahan baku yang sama juga menemukan adanya unsur-unsur lain selain karbon seperti klorin, kalium, oksigen, dan kalsium [27]. Data lengkap tentang unsur-unsur yang terkandung dalam sampel ditunjukkan pada Tabel 3.

Tabel 3. Pesentase kandungan unsur elektroda CMWH

No	Kandungan Unsur	massa (%)	atom (%)
1	Karbon (C)	69.74	88.55
2	Magnesium (Mg)	1.60	1.01
3	Kalium (K)	0.72	0.28
4	Kalsium (Ca)	24.44	9.30
5	Mangan (Mn)	2.31	0.64
6	Tembaga (Cu)	0.36	0.09

7	Strontium (Sr)	0.78	0.14
8	Barium (Ba)	0.05	0.01
	Total	100	100

4.1.6 Analisa Sifat Kristalinitas

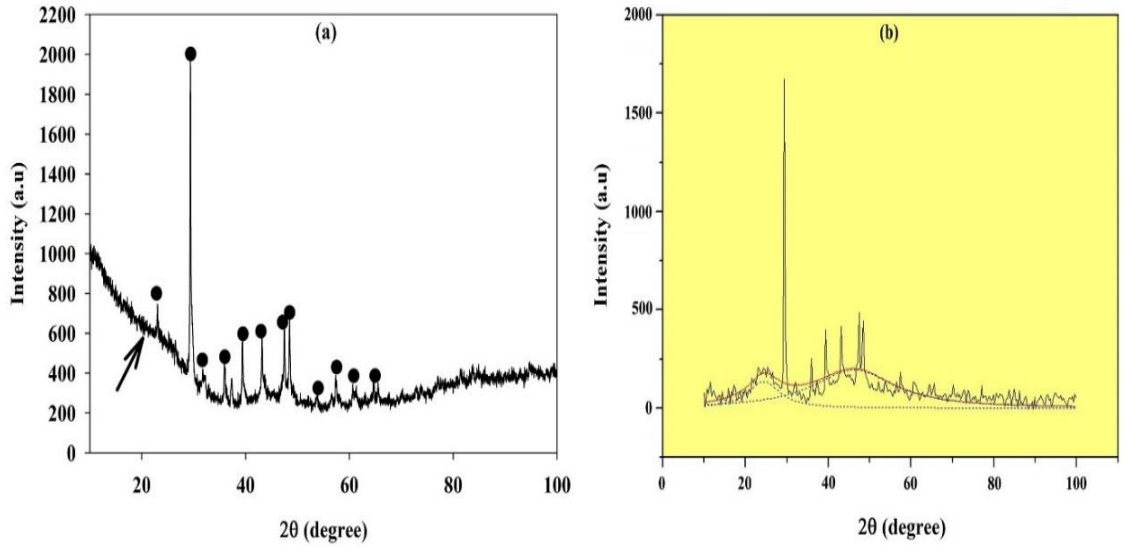

Gambar 9. (a) Pola difraksi sampel CMWH (b) Fittings menggunakan perangkat lunak *Microcal origin*

Kurva hasil karakterisasi difraksi sinar-X untuk sampel CMWH dapat dilihat pada Gambar 9. Data difraktogram XRD menunjukkan hubungan antara intensitas X-ray (au) dan sudut hamburan 2θ (derajat), data ini menunjukkan bahwa ada dua Memperluas puncak pada 2θ sudut 24.429° dan 46.198 °, yang sesuai dengan bidang hamburan d002 dan d100 untuk bahan karbon (Taer *et al.* 2011). Pada Gambar 9a kedua puncak ini tidak terlalu jelas, terutama puncak sesuai dengan sudut 24.429°, setelah melalui proses normalisasi menggunakan perangkat lunak *Microcal origin* kedua puncak ini terlihat lebih jelas dan ditunjukkan pada Gambar 9b. Kedua puncak yang meluas ini menunjukkan sampel CMWH memiliki struktur amorf. Sudut 2θ mengilustrasikan jarak antara lapisan kisi (d_{hkl}) yang dipengaruhi oleh struktur partikel, di mana semakin besar sudut hamburan 2θ semakin kecil d_{hkl} yang dihasilkan. Sampel CMWH memiliki d_{hkl} untuk pesawat d_{002} dan d_{100}, masing-masing 3,64 Å dan 1,96 Å. Ketinggian tumpukan (L_c) setinggi 9.41 Å dan lebar tumpukan (L_a) sebesar 8,01 Å. Selain itu juga ditemukan beberapa puncak tajam dan ditandai dengan tanda bintang pada sudut 23,02°; 29,36°; 31,91°; 35,95°; 37,5°; 39,38°; 43,12°; 47,44°; 53.81°; 56,56°; 57,35°; 60,65° dan 65,52°. Puncak tajam ini menunjukkan adanya senyawa

Kalsium karbonat ($CaCO_3$) dan Selulosa ($C_6H_{10}O_5$). Kehadiran senyawa Kalsium karbonat dan Selulosa dalam sampel CMWH berasal dari bahan yang diserap dari lingkungan dan bahan penyusun untuk tanaman enceng gondok.

4.1.7 Analisa Sifat Kapasitif

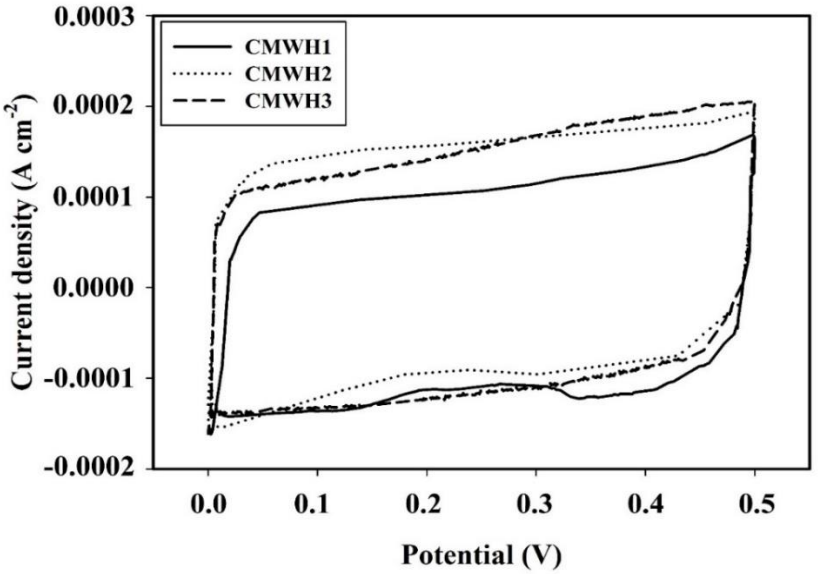

Gambar 10. Kurva CV sel superkapasitor untuk sampel CMWH1, CMWH2, dan CMWH3

Gambar 10 menunjukkan data Cyclic Voltammetry (CV) elektroda CMWH dalam rentang tegangan 0 hingga 0,5 Volt dengan laju scan 1 mV s^{-1}. Kurva CV menunjukkan hubungan antara rapat arus (A cm^{-2}) dengan tegangan (Volt). Kurva CV hampir seperti bentuk persegi panjang, dan ada peningkatan densitas arus pada potensial 0,4 V selama proses pengosongan untuk sampel CMWH1 dan CMWH2. Munculnya peningkatan arus yang hampir menyerupai puncak dalam CMWH1 dan CMWH2 sampel ditunjukkan oleh reaksi oksidasi yang melepaskan sedikit lebih banyak ion. Peningkatan arus muncul pada kedua sampel adalah karena memiliki ketebalan yang lebih kecil dari sampel CMWH3. Reaksi redoks tidak muncul pada elektroda CMWH3 karena ketebalan yang lebih tinggi efek pseudocapacitive ditutupi oleh mekanisme lapisan ganda. Hasil penelitian lain dengan bahan yang sama juga memperoleh keberadaan sifat pseudocapacitive yang diberikan oleh reaksi redoks dan terjadi dalam gugus fungsi oksigen dan nitrogen (Huang *et al.* 2007; Zheng *et al.* 2017).

Sifat-sifat elektroda seperti ketebalan (t), massa (m), laju pemindaian (S), muatan arus (I_c), arus luahan (I_d) dan Kapasitansi spesifik (C_{sp}) untuk tiga sampel elektroda ditunjukkan pada Tabel 4.

Tabel 4. Ketebalan elektroda (t), massa (m), laju pemindaian (S), arus cas (I_c), arus pengosongan (I_d) dan Kapasitansi spesifik (C_{sp}) dari tiga sampel elektroda

Kode sampel	t (mm)	m (g)	S (Vs^{-1})	I_c (A)	I_d (A)	C_{sp} (Fg^{-1})
CMWH1	0.26	0.022	0.001	0.001069	-0.001079	97.64
CMWH2	0.28	0.0235	0.001	0.001389	-0.001159	108.43
CMWH3	0.30	0.028	0.001	0.001550	-0.001153	96.54

Berdasarkan data pada Tabel 4 tertinggi ke kapasitansi spesifik terendah sel supercapacitor adalah 108,43 F g^{-1}, 97,64 F g^{-1} dan 96,54 F g^{-1} untuk CMWH2, CMWH1 dan CMWH3 elektroda, masing-masing. Kapasitansi spesifik dipengaruhi oleh besarnya muatan dan mengeluarkan arus yang diperoleh dari pengukuran CV. Sehingga semakin tinggi arus muatan dan debit yang diperoleh maka semakin tinggi kapasitansi spesifik elektroda.

Tabel 5 menunjukkan perbandingan kapasitansi spesifik elektroda superkapasitor dari enceng gondok dengan metode produksi yang berbeda. Berdasarkan Tabel 5, elektroda karbon dari limbah enceng gondok menunjukkan potensi yang baik untuk digunakan sebagai elektroda karbon dalam perangkat superkapasitor, namun memiliki sifat kapasitif yang relatif lebih rendah.

Tabel 5. Perbandingan kapasitansi spesifik elektroda superkapasitor dari eceng gondok

Materials	Method	C_{sp} (Fg^{-1})	References
Eceng gondok	Aktivasi $ZnCl_2$ dengan variasi suhu karbonisasi (500, 600, 700, 800 and 900 ^oC)	472	(Zhang *et al.* 2012)
Eceng gondok	Metode hidrolisis dan karbonisasi	179.6	(Kurniawan *et al.* 2015)
Eceng gondok	Pra-karbonisasi dan aktivasi KOH	344.9	(Zheng *et al.* 2017)
Eceng gondok	large porous sheet-like carbon materials	273	(Wu *et al.* 2013)
Eceng gondok	Karbon aktif monolit, pra-karbonisasi, aktivasi KOH, aktivasi	108.43	present study

4.2 Elektroda Karbon dari Rumput Purun Tikus

4.2.1 Analisa Densitas

Pengukuran sifat fisis berupa diameter, ketebalan dan massa, kemudian dilanjutkan ke proses karbonisasi dan aktivasi fisika dalam lingkungan gas nitrogen pada suhu 600 ^{o}C dan karbon dioksida pada suhu 900 ^{o}C. Setelah pengolahan data keseluruhan dari sampel, maka langkah selanjutnya adalah pemilihan beberapa sampel saja dengan prioritas agar beberapa sampel pilihan tersebut memperlihatkan penurunan densitas. Selesai seperti tabel diatas, didapati densitas pelet mengalami penurunan setelah diberi perlakuan karbonisasi-aktivasi dan setelah pengeringan via oven 110°C, ukuran diameter dan massanya cukup mengalami penurunan. Penurunan nilai densitas ini dimungkinkan dari pemutusan rantai kompleks ke bentuk yang lebih mendominasi karbon dan pembuangan pengotor selain karbon yang secara beriringan juga memperbesar porositas dari elektroda. Data hasil pengukuran densitas sebelum dan setelah karbonisasi-aktivasi ditampilkan pada Gambar 11 berikut.

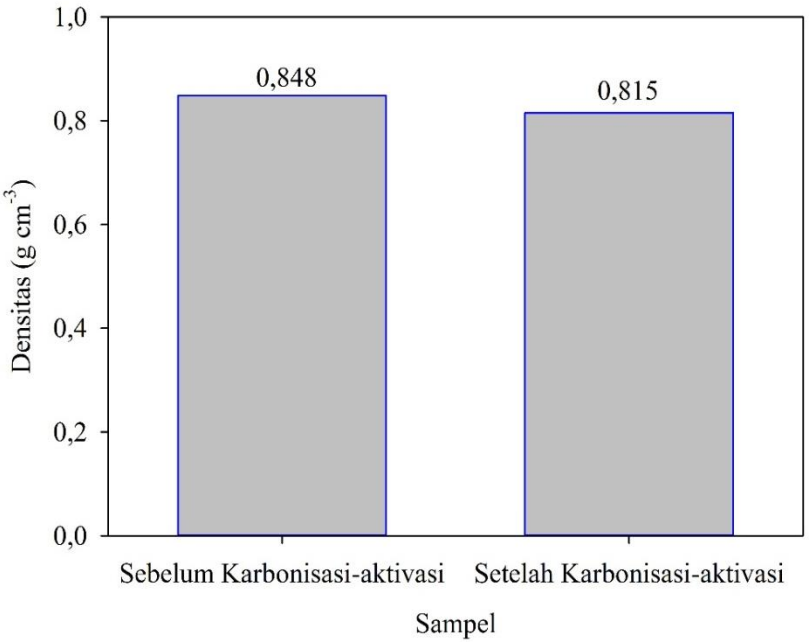

Gambar 11. Densitas elektroda karbon sebelum dan setelah karbonisasi-aktivasi

4.2.2 Analisa Sifat Kapasitif

Data hasil pengukuran menggunakan metode *Cyclic Voltammetry* (CV) ditampilkan pada Tabel 6. Pengukuran sifat elektrokimia menggunakan metode *Cyclic Voltammetry* dilakukan pada beda potensial 0-0,5 V dan variasi scan rate yaitu 1 mV s^{-1}, 2 mV s^{-1}, 5 mV s^{-1}, 10 mV s^{-1}, 20 mV s^{-1}, 50 mV s^{-1} dan 100 mV s^{-1}. Pengukuran

menggunakan metode CV ini bertujuan untuk mengetahui besarnya kapasitansi spesifik sel superkapasitor yang dihasilkan. Secara lengkap, kapasitansi spesifik yang dihasilkan ditampilkan pada Tabel 6 berikut.

Tabel 6. Kapasitansi spesifik elektroda karbon dari rumput purun tikus berdasarkan variasi *scan rate*

Kode sampel	Massa (g)	Ic (A)	Id (A)	Scan rate ($V\ s^{-1}$)	Csp ($F\ g^{-1}$)
GRPT	0,01345	0,000051	-0,000001	0,001	3,87
GRPT	0,01345	0,000032	-0,00001	0,002	1,56
GRPT	0,01345	0,000045	-0,000021	0,005	0,98
GRPT	0,01345	0,000068	-0,000039	0,01	0,79
GRPT	0,01345	0,000113	-0,000074	0,02	0,69
GRPT	0,01345	0,000239	-0,000183	0,05	0,63
GRPT	0,01345	0,00044	-0,00033	0,1	0,57

4.3 Focus Group Discussion (FGD)

Kegiatan Focus Group Discussion (FGD) telah dilakukan dan dilaksanakan pada Hari Sabtu, 20 Oktober 2018 di Hotel Ayola Pekanbaru dengan Tema "Pemanfaatan Tumbuhan Gulma Perairan sebagai Bahan Asal Pembuatan Elektroda Karbon Superkapasitor". Kegiatan ini dihadiri oleh 2 orang Narasumber dari Jurusan Fisika FMIPA Universitas Riau yaitu: Dr. Awitdrus, M.Si selaku Narasumber 1 dan Dr. Erman Taer, M.Si selaku Narasumber 2. Kegiatan ini juga dihadiri oleh Tim Peneliti dari Universitas Islam Negeri Sultan Syarif Kasim Riau dengan ketua Peneliti Dr. Rika, M.Sc. Peserta kegiatan FGD ini juga dihadiri oleh 1 orang Dosen dari Universitas Hasanuddin Makassar dan Mahasiswa/i Universitas Islam Negeri Sultan Syarif Kasim Riau dan Universitas Riau. Kegiatan FGD ini membahas semua permasalahan yang berhubungan dengan piranti penyimpan energi yang biasa disebut dengan Superkapasitor. Dalam kegiatan FGD ini, mahasiswa yang terlibat dalam pelaksanaan penelitian juga mempresentasikan laporan hasil dari kegiatan penelitian yang telah atau sedang mereka kerjakan.

4.4 Luaran yang telah Dicapai

Dari data-data yang telah diperoleh juga telah dilakukan analisa, beberapa data telah dibuat dalam bentuk 2 artikel yang telah diterima dan disajikan pada kegiatan seminar internasional terindeks scopus yaitu "International Conference on Theoritical

an Applied Physics (ICTAP) 2018" yang diselenggarakan oleh Universitas Negeri Medan dan bekerja sama dengan Physical Society of Indonesia (PSI) pada Tanggal 20-21 September 2018. Judul artikel yang diikutkan pada kegiatan ICTAP 2018 ditampilkan pada Tabel 7 berikut.

Tabel 7. Keikutsertaan Kegiatan Seminar Internasional

Kegiatan	Tempat/ Waktu Pelaksanaan	Judul	Status
The 8th International Conference on Theoretical And Applied Physics (ICTAP)	Universitas Negeri Medan, 20-21 Sept 2018	**Natural carbon-metal composite for supercapacitor application**	Sudah dilaksanakan
The 8th International Conference on Theoretical And Applied Physics (ICTAP)	Universitas Negeri Medan, 20-21 Sept 2018	**Producing and characterizing the physical and electrochemical properties of carbon electrodes based on pineapple crown waste: the effect of physics activation time**	Sudah dilaksanakan

Disamping itu melalui dana penelitian dasar cluster madya ini, sebuah publikasi Jurnal International berhasil diterbitkan oleh salah satu anggota tim penelitian ini yang kami anggap hasil luaran tambahan yang harus dilaporkan. Makalah tersebut adalah M. Jelita, R. Taslim, *Conductive-Convective Heat Transfer in an Inclined Enclosure with Vertical Partition*, Advanced Studies in Theoretical Physics, 12 (6), 257-265, penerbit HIKARI Ltd.

Sertifikat:

Physics Society of Indonesia

Certificate

This certificate is awarded to

AGUSTINO

in recognition of his/her valuable contribution as

PRESENTER

In

The 8th International Conferences on Theoretical and Applied Physics (ICTAP) 2018

Grand Inna Hotel Medan, 20-21 September 2018

Indonesian Physical Society Chairman
Prof. Dr. Ing. Mitra Djamal

Indonesian Physical Society of North Sumatera Chairman
Prof. Drs. Motlan, M.Sc., Ph.D

Conference Chairman
Prof. Dr. Nurdin Bukit, M.Si


Physics Society of Indonesia
Certificate
This certificate is awarded to
RIKA TASLIM
in recognition of his/her valuable contribution as
PRESENTER
In
The 8th International Conferences on Theoretical and Applied Physics (ICTAP) 2018
Grand Inna Hotel Medan, 20-21 September 2018
Indonesian Physical Society Chairman
Prof. Dr. Ing. Mitra Djamal
Indonesian Physical Society of North Sumatera Chairman
Prof. Drs. Motlan, M.Sc., Ph.D
Conference Chairman
Prof. Dr. Nurdin Bukit, M.Si

Abstrak:

The 8th International Conference on Theoretical and Applied Physics (ICTAP)
Medan, 20 – 21 September 2018

[A00011]

Naturally Carbon-metal Composite for Supercapacitor Application

R. Taslim[1], A Agustino[2], and E Taer[2]*

[1]Departement of Industrial Engineering, Islamic State University of Sultan Syarif Kasim 28293 Simpang Baru, Riau, Indonesia.
[2]Departement of Physics, University of Riau, 28293, Simpang Baru, Riau, Indonesia

*E-mail: rikataslim@yahoo.com

Abstract—Water hyacinth has been used as the material to produce carbon and metal oxide composite for supercapacitor electrode. The study focus on the effect of electrode thickness variation: (i) 0,26 mm (ii) 0.28 mm, and (iii) 0.30 mm on the electrode density and specific capacitance of the supercapacitor cell. The composite electrode was labeled as CMWH1, CMWH2, and CMWH3. The density of CMWHs electrode are 0.65 g cm-3, 0.66 g cm-3, and 0.70 g cm-3 for CMWH1, CMWH2, and CMWH3 sample respectively. These results show the density is directly proportional to the thickness of the electrode. Electrochemical properties characterization of CMWH electrode was performed using cyclic voltammetry method. The specific capacitance of the CMWH electrode is obtained at 97.64 F g-1, 108.43 Fg-1, and 96.54 Fg-1 for CMWH 1, CMWH2 and CMWH3. Specific capacitance shows the optimum condition at 0.28 mm thickness. The difference trend of specific capacitance with density influenced by pseudocapacitance material properties that exist CMWH electrode. For addition, the TG Analysis, SEM, EDX, and XRD also included in the study.

The 8th International Conference on Theoretical and Applied Physics (ICTAP)
Medan, 20 – 21 August 2018

[A000146]

Producing and characterizing the physical and electrochemical properties of carbon electrodes based on pineapple crown waste: the effect of physics activation time

R Taslim[1], T R Dewi[2], E Taer[2], Apriwandi[2], Agustino[2] and R N Setiadi[2]

[1]Departement of Industrial Engineering, Islamic State University of Sultan Syarif Kasim, 28293 Simpang Baru, Riau, Indonesia
[2]Department of Physics, University of Riau, 28293 Simpang Baru, Riau, Indonesia

Email: rikataslim@gmail.com; erman_taer@yahoo.com;

Abstract–The effect of physical activation time in production of activated carbon electrodes from pineapple crown waste on the physical and electrochemical properties of supercapacitor cells has been demonstrated in this study. The samples were activated in the CO_2 gas environment at a temperature of 900 °C with the activation time varied to 1.5; 2; 2.5 and 3 hours. Physical properties testing showed the activation time of 2.5 hours is the optimum activation time in the producing of carbon electrodes from pineapple crown waste. The optimum conditions are indicated by the minimum condition on the density and microcristalline height, and the maximum condition on specific surface area and carbon content, so it produce higest specific capacitance for supercapacitor cells. The optimum specific capacitance was found as high as 134 F g^{-1}. As a complement also has been analyzed the appearance of the surface morphology of the sample where the electrode is composed of carbon nanofiber with an average diameter of 80-90 nm.

Advanced Studies in Theoretical Physics
Vol. 12, 2018, no. 6, 257 - 265
HIKARI Ltd, www.m-hikari.com
https://doi.org/10.12988/astp.2018.8625

Conductive-Convective Heat Transfer in an Inclined Enclosure with Vertical Partition

Marhama Jelita

Department of Electrical Engineering
Faculty of Science Technology
State Islamic University of Sultan Syarif Kasim
28293 Pekanbaru, Riau, Indonesia

Rika Taslim

Department of Industrial Engineering
Faculty of Science Technology
State Islamic University of Sultan Syarif Kasim
28293 Pekanbaru, Riau, Indonesia

Abstract

Conductive–convective heat transfer in a square enclosure are studied numerically in the present article. The hot and cold walls are making an angle with horizontal direction. The Galerkin weighted residual finite element method has been used to solve the governing partial differential equations. In numerical simulations, the partition thickness, the orientation angle and the Rayleigh number are considered. It is found that the flow circulation decreases with decreasing the orientation angle and the maximum heat transfer rate is obtained near $\varphi = 60°$ for the considered partition thickness.

Keywords: conjugate convection, finite element method, comsol

BAB V

KESIMPULAN

Berdasarkan semua analisis yang telah dilakukan pada Bab IV dapat disimpulkan bahwa:

1. Eceng gondok sebagai bahan asal yang menjanjikan untuk produksi komposit karbon dan oksida logam tanpa penambahan bahan perekat sebagai elektroda pada perangkat superkapasitor.
2. Ketebalan elektroda mempengaruhi densitas elektroda, efeknya pada mekanisme kombinasi EDLC dan pseudocapacitance untuk menemukan kapasitansi spesifik yang optimal.
3. Kapasitansi spesifik optimum sel superkapasitor setinggi 108,43 Fg^{-1} dengan ketebalan elektroda 0,28 mm.
4. Kapasitansi spesifik elektroda karbon dari rumput purun tikus diperoleh sebesar 3,87 F g^{-1}.

DAFTAR PUSTAKA

Burke, A. 2000. Ultracapacitor: why, how, and where is the technology. *Journal of Power Sources* 91:37-50.

Burke, A. 2007. R & D considerations for the performance and application of electrochemical capacitor. *Electrochimica Acta* 53:1083-1091.

Flach, M. and Rumawas, F.1996. Plants Yielding Non-Seed Carbohydrates. PlantResource of South-East Asia (PROSEA). 9:97-100

Gopal , B. 1987. Water Hyacinth. Elsevier Science Publishers, Amsterdam

Kalyani, P and Anitha, A. 2013. Biomass carbon & its prospects in electrochemical energy systems. *International Journal of Hydrogen Energy* 38: 4034-4045.

Nandhini, R., Mini, P.A., Avinash, B., Nair, S.V., and Subramanian, K.R.V. 2012.

Supercapacitor electrodes using nanoscale activated carbon from graphite by ball milling, *Materials Letters* 87: 165-168.

Taer, E., Deraman, M., Talib, I.A., Umar, A.A., Oyama, M. and Yunus, R. M. 2010. Physical, electrochemical and supercapacitive properties of activated carbon pellets from pre- carbonized rubber wood sawdust by CO_2 activation. *Current Applied Physics* 10:1071-1075.

Taer, E., Deraman, M., Talib, I. T., Hashmi, S. A. and Umar, A. A. 2011. Growth of platinum nanoparticles on stanless steel 316L current collector to improve carbon-based supercapacitor performance. *Electrochimica Acta* 56:10217-10222.

Taer, E., Deraman, M., Talib, I.A., Awitdrus, A., Hashmi, S.A. and Umar, A.A. 2011.

Preparation of a highly porous binderless activated carbon monolith from rubber wood sawdust by a multi-step activation process for application in supercapacitor. *International Journal of Electrochemical Science* 6:3301-3315.

Taer, E., Iwantono., Yulita, M., Taslim, R., Subagio, A., Salomo., and Deraman, M. 2013.

Composite electrodes of activated carbon derived from cassava peel and carbon nanotubes for supercapacitor application. Padjadjaran International Physics Symposium. *American Institut of Physics (AIP) conference proceeding series*, 1554: 70-74.

Taer, E., Sugianto., Sumantre, ¸M. A., Taslim, R., Iwantono., Dahlan, D., and Deraman, M. 2014. Eggs Shell Membrane as Natural Separator for Supercapacitor Applications, *Advance Materials Research* 896: 66-69.

Taer, E., Iwantono., Manik, S.T., Taslim, R., Dahlan, D., and Deraman, M. 2014. Preparation of Activated Carbon Monolith Electrodes from Sugarcane Bagasse by Physical and Physical- chemical Activation Process for Supercapacitor Application, *Advance Materials Research* 896: 179-182.

Wang, G., Liang, R., Liu, L., and Zhong, B. 2014. Improving the specific capacitance of carbon nanotubes-basedsupercapacitors by combining introducing functional groups oncarbon nanotubes with using redox-active electrolyte. *Electrochimica Acta*115:183-188.

LAMPIRAN

1. Full Paper ICTAP 2018

Natural carbon-metal composite for supercapacitor application

R Taslim[1*], A Agustino[2] and E Taer[2]

[1]Department of Industrial Engineering, State Islamic University of Sultan Syarif Kasim 28293 Simpang Baru, Riau, Indonesia.
[2]Department of Physics, University of Riau, 28293, Simpang Baru, Riau, Indonesia

[*]E-mail: rikataslim@gmail.com

Abstract. Water hyacinth (eichhornia crassipes) has been used as the material to produce carbon and metal oxide composite for supercapacitor electrode. The study focus on the effect of electrode thickness variation: (i) 0,26 mm (ii) 0.28 mm, and (iii) 0.30 mm on the electrode density and specific capacitance of the supercapacitor cell. The composite electrode was labeled as CMWH1, CMWH2, and CMWH3. The density of CMWHs electrode are 0.65 gcm^{-3}, 0.66 gcm^{-3}, and 0.70 gcm^{-3} for CMWH1, CMWH2, and CMWH3 sample respectively. These results show the density is directly proportional to the thickness of the electrode. Electrochemical properties characterization of CMWH electrode was performed using cyclic voltammetry method. The specific capacitance of the CMWH electrode is obtained at 97.64 Fg^{-1}, 108.43 Fg^{-1}, and 96.54 Fg^{-1} for CMWH 1, CMWH2 and CMWH3. Specific capacitance shows the optimum condition at 0.28 mm thickness. The difference trend of specific capacitance with density influenced by pseudocapacitance material properties that exist CMWH electrode. For addition, the TG Analysis, SEM, EDX, and XRD also included in the study.

1. Introduction

Supercapacitor or Electrochemical Double Layer Capacitor (EDLC) is an energy storage device other than the capacitor, battery and fuel cell [1]. Based on its energy storage mechanism, the supercapacitor is divided into two type: the electrochemical double layer capacitor (EDLC) and pseudocapacitor [2]. The EDLC works based on the formation of ions and electrons pairs at the boundary of electrolyte and electrode. The Electrodes commonly used in EDLC systems is the conductor material with a high surface area such as carbon, while pseudocapacitor works based on oxidation and reduction reactions that appear on certain materials such as metal oxides and conducting polymers. The carbon materials have advantages such as stable in physical and chemical properties, easily controlled pore properties and relatively low production costs [3,4], but produce cells with relatively low capacitance. The pseudocapacitor material has the advantage of high cell capacitance but with relatively high production cost. An alternative to improving supercapacitor cell performance but with low production costs can be developed with a combination of EDLC and pseudocapacitor systems. This combination of working principles can be made by producing carbon composite electrodes and pseudo materials or by preparing EDLC and pseudocapacitance hybrid cell materials. The carbon composite electrodes and material pseudo are a sufficiently effective way to reduce production costs but show good cell

performance. The usual ways of developing composite electrodes are by mixing carbon and pseudo materials such as metal oxides or conduction polymers with the addition of adhesives material. Another common way to use is to grow metal oxide materials in nanostructures on the surface of carbon materials in a variety of shapes and sizes. Metal oxide materials are synthesized from artificial precursors so that production costs are still relatively high. The most commonly used metal oxides are manganese oxide [5], ruthenium oxide [6], nickel oxide [7,8], and cobalt oxide [9,10,11,12].

In this study, the composite electrode of carbon and metal oxide material is made from a natural organic material which naturally contains certain types of metals. The composite electrodes are synthesized from water plants that are easy to absorb some types of metal materials. Water hyacinth is selected as a natural medium that is usually able to absorb several types of metals such as Pb, Cd, Cu, Ni, and Zn [13]. However, the percentage of metal content that can be absorbed by these plants is relatively small so that in the synthesis of composite carbon electrodes, the carbon content of the electrode must be minimized. The focus of this study is to examine the nature of carbon composites and existing metal materials naturally in water hyacinth plants by varying the thickness of the electrodes. The carbon electrodes are produced in pellet form without additional adhesive to maintain the natural conductive properties of carbon materials. In this study electrode shaped pellets with a thickness of 0.26 mm has been able to show the nature of pseudocapacitance. Thus, this study has demonstrated the production of composite electrodes for a combination of EDLC and pseudo material principles through the synthesis of naturally available materials. These results can certainly improve the performance of supercapacitors and reduce production costs.

2. Experimental method

2.1 Preparation of activated carbon

The main material used in this study is water hyacinth. This raw material has been collected then washed to remove any dirt or mud, followed by sun-dried for 48 hours to reduce the moisture content in the sample. After the drying process, water hyacinth is cut into 3 cm in size, then oven-dried at a temperature of 110 °C for 48 hours. The next process is pre-carbonization carried out using the oven at a temperature of 250 °C for 2.5 hours [14,15]. Then, the sample was milled using ball milling for 20 hours in order to obtain sample size less than 8 μm. The sample was then chemically activated using KOH activator at concentration 0.2 M. The KOH activators have been used in the study that we have reported previously [14,16,17,18,19]. The activated sample was molded to pellet form at a diameter of 19 mm using the Hydraulic press at 8 tons [15,20]. The carbonization process is carried out at a temperature of 600 °C in the N_2 gas environment [15,19,21,22] and followed by physical activation using CO_2 gas at a temperature of 850 °C for 2 hours. This physical activation time was in accordance with the activation time that we reported previously [14,19,23,24]. All activated carbon samples are polished to the desired thickness and washed until the washing water becomes neutral.

2.2 Manufacture of supercapacitor cells

A pair of activated carbon pellets made from water hyacinth is used as electrodes in the manufacture of sandwich-shaped supercapacitor cells. Another material used is a pair of 316L stainless steel tape as a current collector, a duck eggshell membrane is used as a separator and 1 M sulfuric acid solution is used as the electrolyte. The carbon electrodes were immersed using 1 M H_2SO_4 electrolyte solution for 48 hours, then assembled into supercapacitor cells as we previously reported [16,20,21].

2.3 Characterization of carbon electrodes

The physical properties tested on carbon electrode from water hyacinth include thermal properties, density, surface morphology, elemental content and crystalline degree. The thermal properties test is performed using the Thermogravimetric Analysis (TGA) method. The TGA testing was performed in an N_2 gas environment to a temperature of 600 °C at a temperature scan rate of 10 °C min^{-1} using Netzsch derivatograph (STA 449 F1 Jupiter instrument). The density of carbon electrodes is obtained from measurements of mass, diameter, and thickness of each sample before and after the

carbonization-activation process is carried out. The activated carbon electrode varied for three different thickness by the polished process. The N_2 gas adsorption-desorption testing was carried out using the Brunauer Emmet Teller method using Quantachrome Instruments version 11.0 for analysis of the specific surface area of carbon electrode sample. Morphological structure testing and element content were carried out using Scanning Electron Microscopy and energy dispersive X-ray using JEOL-JSM 6510 LA instrument. The X-ray diffraction test was used to determine the lattice and crystalline phase parameters in carbon samples using X-pert powder panalytical diffractometer with CuKα ray source, with a wavelength of 0.154 nm and the diffraction angle used was 2θ ie at an angle range of 10-100°.

2.4 Electrochemical properties

The measurement of electrochemical properties of supercapacitor cells was performed using Cyclic Voltammetry (CV) method. This measurement uses the Physics CV UR Rad-Er 5841 and calibrated with VersaStat II Princeton Applied Research calibrator standard instrument. This measurement was carried out at a potential window range of 0 V-0.5 V and a scan rate of 1 mVs^{-1} [18,22,25]. The specific capacitance (C_{sp}) was calculated using the following equation:

$$C_{sp} = \frac{I_c - I_d}{Sxm} \quad (1)$$

Where I_c is the charging current (A), I_d is the discharge current (A), S is the scan rate and m is the mass of the electrode.

3. Results and Discussion

3.1 Thermogravimetry analysis

Thermal properties were analyzed by Thermogravimetric (TG) and Differential Thermal Termographymetry (DTG). The parameters studied was changes in the sample mass to the temperature change. The DTG is used to measure the rate of change in sample mass against temperature rise. Both of these analyzes were carried out at a temperature range of 30-600 °C at a heating rate of 10 °C min^{-1} in the N_2 gas environment. The mass of sample for thermal analysis is 7.199 mg. The thermal properties data for pre-carbonize water hyacinth samples is shown in Figure 1.

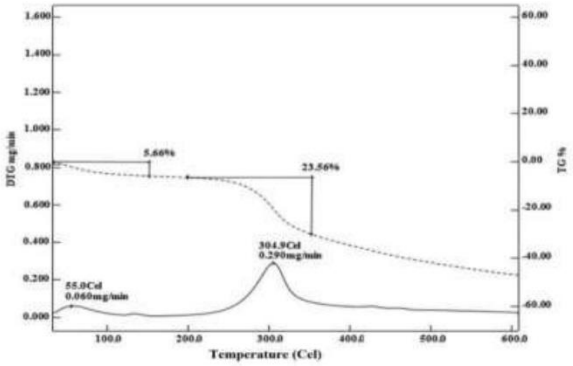

Figure 1. The TG, and DTG profile curves for water hyacinth samples

Figure 1 shows the profile of the sample mass change in the percent (%) to the temperature (C). The TG curve of Figure 1 was represented by dashed line. The TG data shows the pattern of sample mass reduction when the temperature is raised. Significant mass reductions occurred in the temperature range of 30-151 °C, 210-353 °C and subsequently the sample mass decreased gradually from a temperature of 353-600 °C. The first mass reduction in the first temperature range of 30-151 °C as high as 5.66% affected by the release of water content [26,27,28]. The second one at a temperature range of 210-353 °C amount 23.56% is influenced by the simultaneous decomposition of cellulose and hemicellulose [29], whereas in the third stages the sample mass reduction occurs due to lignin decomposition [30,31].

The DTG curve is indicated by the solid line in Figure 1, the shape of the curve is marked by the presence of two peaks at temperatures of 55 °C and 304.9 °C, respectively. This peak shows in the optimum mass reduction rate to the temperature. The first peak shows the optimum mass degradation rate in the temperature range 30 -151 °C by 0.060 mg min^{-1}, while at the second peak shows the optimum mass degradation rate experienced by the sample is 0.290 mg min^{-1} and occurs in the temperature range 210-353 °C. This temperature of 304.9 °C shows the optimum mass degradation rate which is the maximum decomposition of the basic elements of the sample to increase the carbon elements. This temperature is then chosen as the resistance temperature in the sample carbonization process to ensure a higher level of carbon purity.

3.2 Mass, diameter, thickness and density of the electrode

The measurements results of mass, diameter, thickness, and density of the electrodes before and after carbonization-activation, and after the polishing process are shown in Table 1. The mass, diameter, thickness, and density of the electrode before the carbonization-activation process is almost the same, this result was reasonable because of the same sample treatment while the difference in result is due to the pre-carbon powder being wasted during the molding process at a compression pressure. The mass, diameter, thickness, and density of CMWH electrodes after the carbonization-activation process have decreased due to the release of non-carbon materials during the carbonization-activation process [32]. The CMWH electrode mass after the polishing process shows a difference, this is due to the difference in electrode thickness, the greater electrode thickness will result in a higher electrode mass. While the diameter of the electrode after the polishing process also has a different, this is due to electrode erosion during polishing. The different in electrode density after polishing because of the difference in thickness for every sample. The highest density was found by the CMWH3 sample with an electrode thickness of 0.30 mm which is 0.70 gcm^{-3}, while the smallest density value is CMWH1 sample with a thickness of 0.26 mm which is 0.65 gcm^{-3}. This result is influenced by changes in mass and diameter due to the polishing process.

Tabel 1. Mass (g), diameter (mm), thicness (mm), and density (gcm^{-3})

Sample codes	Before carbonization-activation				After carbonization-activation				After polishing			
	m	d	t	ρ	m	d	t	ρ	M	d	t	ρ
CMWH1	0.582	19.72	0.235	0.81	0.192	13.58	0.162	0.82	0.022	12.90	0.26	0.65
CMWH2	0.59	19.95	0.243	0.78	0.195	13.85	0.161	0.80	0.0235	12.68	0.28	0.66
CMWH3	0.573	19.78	0.234	0.80	0.213	14.29	0.168	0.79	0.028	13.01	0.30	0.70

3.3 N_2 gas adsorption-desorption isotherms Analysis

Figure 2a shows the N_2 gas adsorption-desorption isotherm data on the carbon electrodes sample, this data shows the relationship between the adsorption-desorption volume to the relative pressure (P/P_0). The N_2 gas adsorption-desorption model shown in Figure 2a was type IV according to the IUPAC classification although there is a slight difference in the relatively large pressure conditions. The assertion of type IV is shown by an increase in absorption volume at a relative pressure of 0.4.

Figure 2b shows the relationship between dV/dr (d) to the sample pore diameter using the BJH method. The BJH method was used to see the pore distribution from the range of 3.5 to 40 nm. It can be seen that the decrease in pore volume occurs in the pore diameter range of 3.5-7.0 nm and shows the maximum pore volume at 3.5 nm diameter of 0.001 $cm^3nm^{-1}g^{-1}$. The maximum absorption volume shows that the dominant sample pore diameter is in the range mesoporous. The assertion of type IV adsorption-desorption data is strengthened with an average of BJH pore diameter of 3.5911 nm, which shows the average pore diameter of the sample was in the mesoporous group corresponding to type IV characteristics [33]. Senthilkumar et al. 2013 with the same material also obtained a pore diameter in the mesoporous range [33].

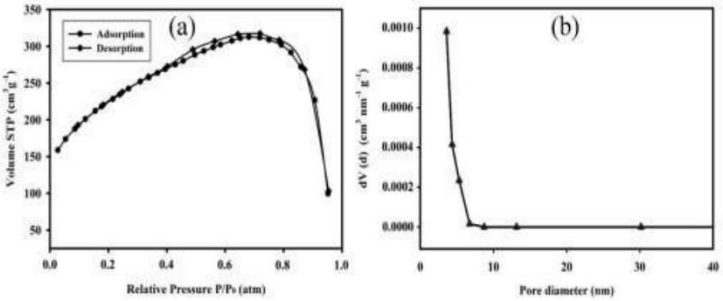

Figure 2. (a) N_2 gas adsorption-desorption isotherm and (b) pore size distributions

The specific surface area data (S_{BET}), BJH surface area, BJH volume, and diameter are shown in Table 2. Zhang et al, 2012 and Kurniawan et al, 2015 also studying the same material obtained specific surface area (S_{BET}) of 579.94 m^2g^{-1} [34] and 761 m^2g^{-1} [35].

Table 2. The N_2 gas absorption measurements result from CMWH sample

Sample	S_{BET} (m^2 g^{-1})	S_{BJH} (m^2 g^{-1})	V_{BJH} (cm^3 g^{-1})	D_{BJH} (Å)
CMWH	776.213	130.548	0.133	35.911

3.4 Scanning electron microscopy analysis

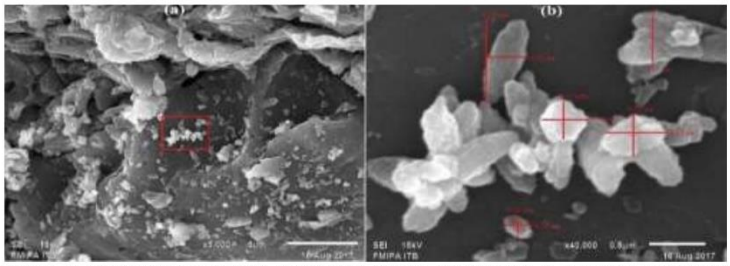

Figure 3. The SEM micrograph of CMWH sample (a) CMWH at magnification 5000x (b) CMWH at 40000x magnification

Figures 3a and 3b show the SEM micrograph CMWH sample at 5000x and 40000x magnification. Figure 3a with a shows the surface morphology of CMWH which is shaped like a lump and is

dominated by black color which is assosiated with carbon particle and also seen particles that are smooth white indicating other elements than carbon. At this magnification, there is also no macropore on the surface of the CMWH sample. While Figure 3b is an enlargement in the area marked in red in Figure 3a. These smooth particles have a shape that tends to be regular with an oval shape dominated by a length of 0.44 μm and 0.38 μm wide.

3.5 Energy dispersive x-ray analysis

The EDX test results of the sample are shown in Figure 4 which were selected in an area of 15 μm^2 which is indicated by a green box in the SEM image that is inserted in the upper right side. The EDX data shows the elements contained in CMWH samples namely carbon (C), magnesium (Mg), potassium (K), calcium (Ca), manganese (Mn), copper (Cu), strontium (Sr) and barium (Ba). The content of the constituent elements of the sample is dominated by carbon and calcium at 0.277 keV and 3.690 keV indicated by the highest count, respectively. The mass and atomic percentage were 69.74%, 88.55%, for carbon and 24.44%, 9.30% for calcium, respectively. The other elements such as Magnesium, potassium, manganese, copper, strontium, and barium with energies of 1.253 keV, 3.312 keV, 5.894 keV, 8.040 keV, 1.806 keV and 4.464 keV, respectively. The other studies with the same raw material also found the presence of other elements than carbon such as chlorine, potassium, oxygen, and calcium [27]. The complete data on the elements contained in the sample are shown in Table 3.

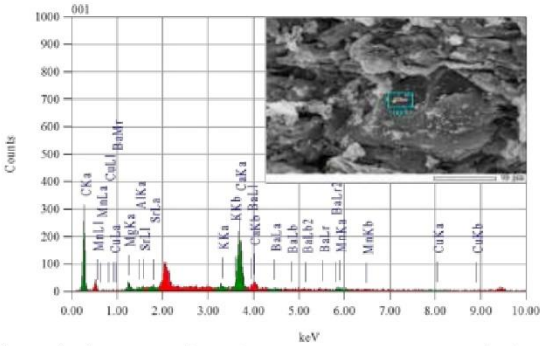

Figure 4. The Energy dispersive X-rays measurement result data of CMWH samples

Table 3. Percentage of elements contained in the CMWH electrode

No	Elements	mass (%)	atom (%)
1	Carbon (C)	69.74	88.55
2	Magnesium (Mg)	1.60	1.01
3	Pottasium (K)	0.72	0.28
4	Calsium (Ca)	24.44	9.30
5	Mangan (Mn)	2.31	0.64
6	Copper (Cu)	0.36	0.09
7	Strontium (Sr)	0.78	0.14
8	Barium (Ba)	0.05	0.01
	Total	100	100

3.6 X-ray diffraction analysis

The curve of X-ray diffraction characterization results for CMWH sample can be seen in Figure 5. The XRD diffractogram data shows the relationship between X-ray intensity (a.u) and scattering angle of 2θ (degrees), this data shows that there are two broadening peaks at 2θ angles of 24.429° and 46.198°, which correspond to the scattering plane of d_{002} and d_{100} for carbon materials [36]. In Figure 5a these two peaks are not very clear, especially the peak corresponds to the angle of 24.429°, after going through the process of normalization using the Microcal origin software these two peaks look more clearly and are shown in Figure 5b. Both of these broadening peaks indicate the CMWH sample has an amorphous structure. The angle 2θ illustrates the distance between the lattice layers (d_{hkl}) which is affected by the structure of the particle, where the greater of the scattering angle 2θ the smaller the resulting d_{hkl}. The CMWH sample has d_{hkl} for planes d_{002} and d_{100}, respectively 3.64 Å and 1.96 Å. The stack height (L_c) as high as 9.41 Å and stack width (L_a) of 8.01 Å. In addition also found some sharp peaks and are marked with an asterisk at an angles of 23.02°; 29.36°; 31.91°; 35.95°; 37.5°; 39.38°; 43.12°; 47.44°; 53.81°; 56.56°; 57.35°; 60.65° and 65.52°. This sharp peak indicates the presence of Calcium carbonate ($CaCO_3$) and Cellulose ($C_6H_{10}O_5$) compounds. The presence of Calcium carbonate and Cellulose compounds in the CMWH sample is derived from materials absorbed from the environment and the constituent materials for water hyacinth plants.

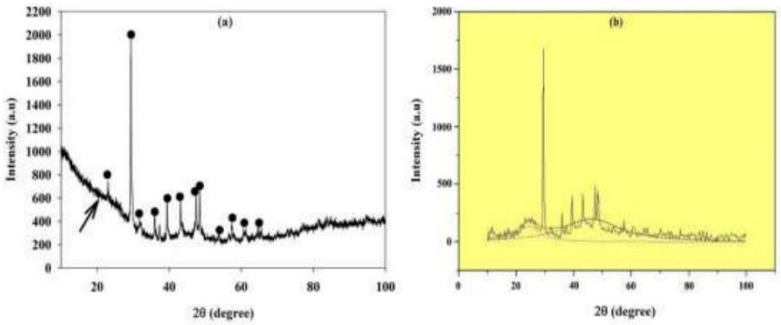

Figure 5. (a) CMWH sample X-ray diffraction pattern, (b) Fittings using microcal origin software

3.7 Cyclic Voltammetry (CV) Analysis

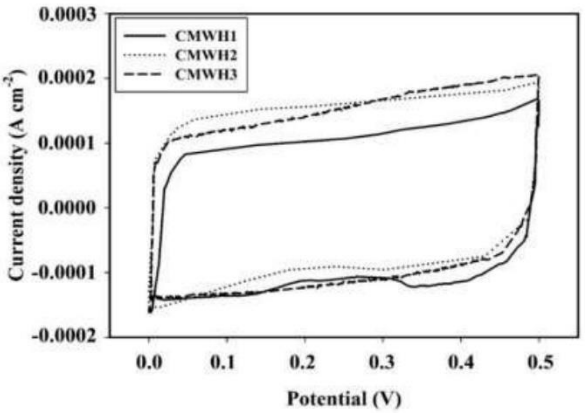

Figure 6. The CV curve of supercapacitor cell for CMWH1, CMWH2, and CMWH3 samples

Figure 6 shows Cyclic Voltammetry (CV) data CMWH electrode in the voltage range of 0 to 0.5 Volt with a scan rate of 1 mVs^{-1}. The CV curve shows the relationship between current density (Acm^{-2}) to the voltage (Volt). The CV curve has almost like a rectangular shape, and there is an increase in the current density at a potential of 0.4 V during the discharge process for CMWH1 and CMWH2 samples. The appearance of the current increase which almost resembles the peaks in CMWH1 and CMWH2 samples are indicated by an oxidation reaction which releases a little more ions. The increasing current in both samples was due to its having a smaller thickness than the CMWH3 sample. The redox reaction doesn't appear on the CMWH3 electrode because of the higher thickness the pseudocapacitive effect covered by a double layer mechanism. The results of other studies with the same material also obtained the presence of pseudocapacitive properties given by redox reactions and occur in oxygen and nitrogen functional groups [37,38].

The electrode properties such as thickness (t), mass (m), scan rate (S), current charge (I_c), Current discharge (I_d) and Specific capacitance (C_{sp}) for three electrode samples are shown in Table 4.

Table 4. The electrode thickness (t), mass (m), scan rate (S), charge current (I_c), discharge current (I_d) and Specific capacitance (C_{sp}) of three electrode samples

Sample codes	t (mm)	m (g)	S (Vs^{-1})	I_c (A)	I_d (A)	C_{sp} (Fg^{-1})
CMWH1	0.26	0.022	0.001	0.001069	-0.001079	97.64
CMWH2	0.28	0.0235	0.001	0.001389	-0.001159	108.43
CMWH3	0.30	0.028	0.001	0.001550	-0.001153	96.54

Based on the data in Table 4 the highest to the lowest specific capacitance of supercapacitor cells were 108.43 Fg^{-1}, 97.64 Fg^{-1} and 96.54 Fg^{-1} for CMWH2, CMWH1 and CMWH3 electrodes, respectively. The specific capacitance is affected by the magnitude of the charge and discharges current obtained from the CV measurement. So that, the higher the charge and discharge current was obtained then the higher electrode specific capacitance.

Table 5 shows the comparison of the specific capacitance of supercapacitor electrodes from water hyacinth with the different production methods. Based on Table 5, carbon electrode from water hyacinth waste indicates good potential for use as carbon electrodes in supercapacitor devices, however has relatively lower capacitive properties.

Table 5. Comparison of the specific capacitance of supercapacitor electrodes from water hyacinth

Materials	Method	C_{sp} (Fg^{-1})	References
Water hyacinth	$ZnCl_2$ activation at different carbonization temperatures (500, 600, 700, 800 and 900 °C)	472	[34]
Water hyacinth	Subcritical water hydrolysis and carbonization methods	179.6	[35]
Water hyacinth	pre-carbonization and KOH activation	344.9	[38]
Water hyacinth	large porous sheet-like carbon materials	273	[39]
Water hyacinth	Activated carbon monolit, pre-carbonization, KOH activation, CO_2 activation	108.43	present study

5. Conclusion

Based on all data analysis it can be concluded that water hyacinth as a promising raw material for the production of carbon and metal oxide composites without addition of adhesive material as electrodes on supercapacitor devices. The thickness of the electrode affects the electrode density, its effect on the combination mechanism EDLC and pseudocapacitance to find the optimum specific capacitance. The optimum specific capacitance of supercapacitor cells as highs as 108.43 Fg^{-1} with electrode thickness of 0.28 mm.

Acknowledgements

We would like to thank the Rector of the State Islamic University of Sultan Syarif Kasim Riau for the finansial support by using the basic cluster of scientific integration 2018 with the Principal researcher of Dr. Rika, S.Si., M.Sc with the project titled "Utilization of aquatic weed plants as the raw material for the production of supercapacitor electrodes" with contract number: 0935/R/2018.

References

[1] Burke A 2000 *J. Power Sources* **91** 37
[2] ZhangY, Feng H, Wu X, Wang L, Zhang A, Xia T, Dong H, Li X and Zhang L 2009 *Int. J. Hydrogen Energy* **34** 4889
[3] Pandolfo A G and Hollenkamp A F 2006 *J. Power Sources* **157** 11
[4] Frackowiak E and Beguin F 2001 *Carbon* **39** 937
[5] Huang Q, Wang X. and Li J 2006 *Electrochim. Acta* **52** 1758
[6] Mondal S K and Munichandraiah N 2008 *J. Power Sources* **175** 657
[7] Cheng J, Cao G P and Yang Y S 2006 *J. Power Sources* **159** 734
[8] Xu J, Gu X, Cao J, Wang W and Chen Z 2012 *J. Solid State Electrochem.* **16** 2667
[9] Svegl F, Orel B, Hutchins M G and Kalcher K 1996 *J. Electrochem. Soc.* **143** 1532
[10] Wei T Y, Chen C H, Chang K H, Lu S Y and Hu C C 2009 *Chem. Mater.* **21** 3228
[11] Li Y, Huang K, Yao Z, Liu S and Qing X 2011 *Electrochim. Acta* **56** 2140
[12] Ali M A G, Fouad A O, Makhlouf A S and Chongm F K 2014 *J. Solid State Electrochem.* **18** 2505
[13] Mahmood T, Malik S A and Hussain S T 2010 *Bioresour.* **5** 1244
[14] Taer E, Susanti Y, Awitdrus, Sugianto, Taslim R, Setiadi R N, Bahri S, Agustino, Dewi P, and Kurniasih B 2018 *AIP Conf. Proc.* **1927** 030016-1
[15] Taer E, Dewi P, Sugianto, Syech R, Taslim R, Salomo, Susanti Y, Purnama A, Apriwandi, Agustino and Setiadi R N 2018 *AIP Conf. Proc.* **1927** 030026-1
[16] Farma R, Deraman M, Omar R, Awitdrus, Ishak M M, Taer E, and Talib I A 2011. *AIP Conf.*

Proc. **1415** 180
[17] Taer E, Iwantono, Manik S T, Taslim R, Dahlan D, and Deraman M 2014 *Adv. Mater. Res.* **896** 179
[18] Taer E, Mustika W S, Agustino, Fajarini, Hidayu N. and Taslim R 2017 *IOP Conf. Ser.: Earth Environ. Sci.* **58** 012065
[19] Taer E, Kurniasih B, Sari F P, Zulkifli, Taslim R, Sugianto, Purnama A, Apriwandi and Susanti Y 2018 *AIP Conf. Proc.* **1927** 030006-1
[20] Taer E, Deraman M, Talib I A, Umar A A, Oyama M and Yunus R M 2010 *Curr. Appl. Phys.* **10** 1071
[21] Taer E, Sugianto, Sumantre M A,Taslim R, Iwantono, Dahlan D, and Deraman M 2014 *Adv. Mater. Res.* **896** 66
[22] Taer E, Apriwandi, Yusriwandi, Mustika W S, Zulkifli, Taslim R, Sugianto, Kurniasih B, Agustino and Dewi P 2018 *AIP Conf. Proc.* **1927** 030036-1
[23] Taer E, Deraman M, Taslim R, and Iwantono 2013 *AIP. Conf. Proc.* **1554** 37
[24] Taer E, Taslim R, Mustika W S, Kurniasih B, Agustino, Afrianda A, and Apriwandi 2018 *Int. J. Electrochem. Sci.* **13** 8428
[25] Taer E, Taslim R, Aini Z, Hartati S D and Mustika W S 2017 *AIP. Conf. Proc.* **1801** 040004-1
[26] Luo G, Strong J, Wang H, Ni W, Shi W 2011 *Bioresour. Technol.* **102** 6990
[27] Madrid J F, Nuesca G M and Abad L C 2013 *Rad. Phys. Chem.* **85** 182
[28] Gao Y, Wang X, Wang J, Li X, Cheng J, Yang H and Chen H 2013 *Energy* **58** 376
[29] Yao F, Wu Q, Lei Y, Guo W, Xu Y, 2008 *Pol Deg. Stability* **93** 90
[30] Fisher T, Hajaligol M, Waymack B, Kellogg D 2002 *J. Anal. Appl. Pyrol.* **62** 331
[31] Harun M Y, Radiah A B D, Abidin Z Z and Yunus R 2011 *Bioresour. Technol.* **102** 5193
[32] Farma R, Deraman M, Awitdrus, Talib I A, Omar R, Manjunatha J G, Ishak M M, Basri N H, and Dolah B N M 2013 *Int. J. Electrochem. Sci.* **8** 257
[33] Senthilkumar S T, Selvan R K, Lee Y S and Melo J S 2013 *J. Mater. Chem. A* **1** 1086
[34] Zhang X, Wang X, Su J, Wang X, Jiang L, Wu H and Wu C 2012 *J. Power Sources* **199** 402
[35] Kurniawan F, Wongso M, Ayucitra A, Soetaredjo F E, Angkawijaya A E, Ju Y -H and Ismadji S 2015 *J. Taiwan Inst.Chem. E.* **47** 197
[36] Taer E, Deraman M, Thalib I A, Awitdrus A, Hasmi S A, Umar A A 2011 *Int. Journal Electrochem. Sci.* **6** 3301
[37] Huang C W, Wu Y T, Hu C C and Li Y Y 2007 *J. Power Sources* **172** 460
[38] Zheng K, Li Y, Zhu M, Yu X, Zhang M and Cheng J 2017 *J. Power Sources* **366** 270
[39] Wu X, Hong X, Luo Z, Hui K S, Chen H, Wu J, Hui K N, Li L, Nan J, Zhang Q 2013 *Electrochim. Acta* **89** 400

Producing and characterizing the physical and electrochemical properties of carbon electrodes based on pineapple crown waste: the effect of physics activation time

R Taslim[1], T R Dewi[2], E Taer[2], A Apriwandi[2], A Agustino[2] and R N Setiadi[2]

[1]Departement of Industrial Engineering, Islamic State University of Sultan Syarif Kasim, 28293 Simpang Baru, Riau, Indonesia
[2]Department of Physics, University of Riau, 28293 Simpang Baru, Riau, Indonesia

Email: rikataslim@gmail.com; erman_taer@yahoo.com;

Abstract. The effect of physical activation time in production of activated carbon electrodes from pineapple crown waste on the physical and electrochemical properties of supercapacitor cells has been demonstrated in this study. The samples were activated in the CO_2 gas environment at a temperature of 900 °C with the activation time varied to 1.5; 2; 2.5 and 3 hours. Physical properties testing showed the activation time of 2.5 hours is the optimum activation time in the producing of carbon electrodes from pineapple crown waste. The optimum conditions are indicated by the minimum condition on the density and microcristalline height, and the maximum condition on specific surface area and carbon content, so it produce higest specific capacitance for supercapacitor cells. The optimum specific capacitance was found as high as 134 Fg^{-1}. As a complement also has been analyzed the appearance of the surface morphology of the sample where the electrode is composed of carbon nanofiber with an average diameter of 90-164 nm.

1. Introduction

Electrochemical double layer capacitors (EDLC) are energy storage devices consisting of porous carbon electrodes, electrolyte, separator and current collectors [1]. Energy storage occurs because of the presence of ion and electron layers formed in the micro pore of the carbon electrode. The more ion pairs and electrons that form the greater the energy that can be stored. The formation of ion and electron pairs is affected by the number of micro pores available in an electrode. Micro pores electrodes are relate to the materials and activation process. Power is the main factor in the performance of EDLC devices other than energy. Power is related to the speed of ion diffusion process into the pores of the electrode to form ion-electron pairs. The pace of ion diffusion is clearly related to the shape of the electrode constituent material and pore size. In the last decade, the shape of electrode constituent materials becomes a fairly extensive study [2]. Various shape of electrode constituent materials have been reported such as cubic [3,4,5], spherical, flat, fiber [6,7] provided in nano or micro sizes. The shape of fiber is one of the most developed forms due to several advantages such as hollow pores and good electrical conductivity [7]. The selection of the original material in the prepare of carbon fiber is one of the interesting research focuses. Production costs are a major consideration in the selection of original material. Biomass promises low production costs, abundant availability and

also being a by-product in the agricultural industry [8]. Some biomass materials as originating materials for the prepared of carbon fiber electrodes that have been reported, such as banana stems [9], coconut husk [7], oil palm empty fruit bunches [10], etc. Different biomass materials provide different sizes of fiber diameters. Pineapple crowns are one of the biomass that contains fiber. The fiber sizes vary in nano to micro meters. Indonesia is one of the pineapple producing countries with production reaching 1.73 ton in the year 2015 [11]. In this research, a simple method is used to produce carbon fiber electrodes from pineapple crown waste as supercapacitor electrodes. Carbon electrodes are provided without additional adhesives and are activated conventionally using KOH and CO_2 gas. The results showed that the carbon electrode from pineapple crwon produced supercapacitor cells as high as 134 F g^{-1} and found to contain dominant carbon fiber with a diameter size an average of 90-164 nm.

2. Experimental Method

2.1. Preparation of carbon electrode

The biomass used as raw material in this study is pineapple crown. The production of activated carbon from the pineapple crown uses the method previously reported [12]. Pre-carbonization was carried out by heating at a temperature of 250℃ for 2.5 hours. The pre-carbonization process will cause the sample color to be dark-brown and self-adhesive in the sample will appear. The sample is smoothed with a ball milling instrument. The ball milling process is carried out with the aim to produce finer the dark-brown pineapple crown powder. The dark-brown pineapple crown powder was activated using KOH activator with a ratio of 1:1. The sample powder is converted into a monolithic or pellet form by using a Hydraulic Press system [13]. Pyrolysis processes such as carbonization and physical activation are carried out using a one-step integrated method [14]. Carbonization begins with the flow of nitrogen gas (N_2) with a gas flow rate of 1.5 L min^{-1} at a temperature of 600℃ and followed by physical activation by flowing CO_2 gas at a temperature of 900℃. Physical activation time were varied at 1.5, 2, 2.5 and 3 hours. Based on this time variation, each sample is labeled AC-1.5, AC-2.0, AC-2.5 and AC-3.0. Then carbon pellets were wash until the washing water becomes neutral [15]. The preparation of supercapacitor cells in two-electrode system consisting of carbon electrodes, separator, electrolytes and current colectors [1,16]. Separator used is the duck eggshell membrane [17] and H_2SO_4 solution as electrolyte [18].

2.2. Characterization of physical and electrochemical properties.

Measurement of physical properties of pineapple crowns carbon electrodes included of density, crystalline structure, surface morphology and component elements of carbon electrodes while the characterization of electrochemical properties included of capacitive properties of supercapacitor cells. Density is calculated by measuring the mass and volume of the electrode. Analysis of surface morphology and element content of carbon electrodes using Scanning Electron Microscophy (SEM) and Energy Dispersive X-ray Spectroscopy (EDX) methods with Jeol JSM 6510 LA instrument. The crystallinity is caraterized by X-ray Diffraction method with X-Pert Powder panalyticsl instrument. Capacitive properties testing using the Cyclic Voltammetry method with the Physics CV UR Rad-Er 5841 which is controlled by cyclic voltammetry CV v6 software.

3. Result and Discussion

3.1. Density Analysis

Comparison of density before and after pyrolysis for carbon electrode samples can be seen in Figure 1. Figure 1 is shown pre-carbonize sample before the pyrolysis process have an average density of 0.932 gcm^{-3}. After pyrolysis process shows the effect of activation time on the density of carbon electrodes, where the density decreases with the addition of activation time (from 0.924 gcm^{-3} at a AC-1.5 sample to 0.625 gcm^{-3} at a AC-2.5 sample). This density reduction is affected by the release of pollutant components such as volatiles which cause pore formation. An increasing in activation time causes the more effective reaction between carbon and CO_2 so that the density decreases. After the addition of activation time of 2.5 hours the sample had an increase in density of 15.2%. This is indicated by at 3

hours, the sample has suffered decay to the particles and the pores are not formed in optimum condition. All the density data, the lowest density occurs at 2.5 hours activation time, this 2.5 hours activation time is chosen to be the best activation time to produce activated carbon from the pineapple crown waste.

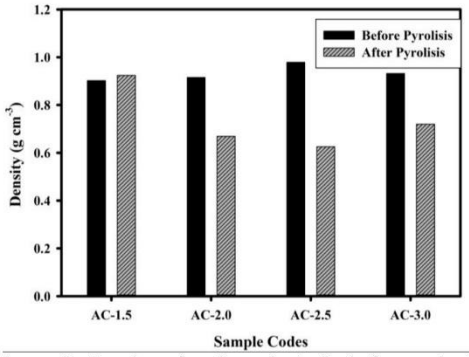

Figure 1. Density of carbon electrode before and after pyrolisis process

3.2. Scanning Electron Microscopy Analysis

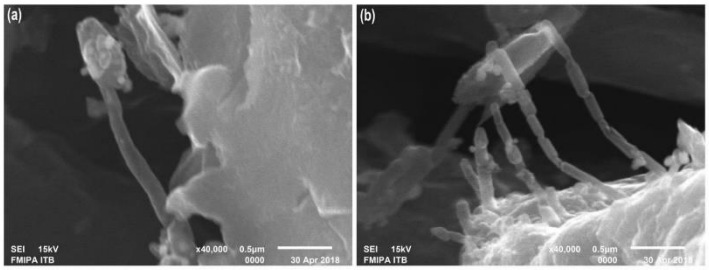

Figure 2.SEM micrographs with a magnification of 40000 times for a) AC-2.0; b) AC-2.5

Characterization of Scanning Electron Microscopy is used to determine the morphological surface structure of activated carbon electrode. Morphological surface structure of pineapple crown activated carbon for AC-2.0 and AC-2.5 samples with a magnification of 40,000 times are shown in Figure 2. Figure 2 (a) shows the results of SEM AC-2.0 carbon electrodes have pores between particles that look elongated and irregular. In addition, there is also a presence of nanofiber structures, where the average fiber diameter range of 164 nm. Figure 2 (b) presents the SEM results for AC-2.5 with larger pores between particles. The resulting nanofiber structure is more clearly visible with a relatively smaller size with a sample diameter in range of 83 to 90 nm. The size diameter in this study are same carbon fiber electrode with the diffrent biomass such as banan stems in range 42-131 nm [9]. The particles formed are affected by the activation time, increasing activation time results in a finer fiber size. This is indicated because the addition of activation time provides a longer chance for the process of carbon and CO_2 reactions so that the carbon chain termination will increase. Termination of the

carbon chain results in cracks and faults in larger particles, increasing activation time also causes faster particle movements resulting in larger collisions between particles. Collisions between particles will cause carbon particles to split into smaller parts.

3.3. Energy Dispersive X-ray (EDX) Analysis

The EDX Characterization was carried out to prove the presence of carbon on the electrode sample made from pineapple crown waste. EDX analysis strengthens the data that has been obtained from the SEM and XRD characterization that will be analized in the next subsection. EDX analysis produces data in a percentage of the quantity of elements of activated carbon samples. Based on the data in Table 1, the element quantities of the carbon electrode consist of carbon (C), oxygen (O), magnesium (Mg), silicon (Si), phosphorus (P), Potassium (K) and calcium (Ca). The element quantities are dominated by carbon with a range of 92% to 94%. These results prove that the samples dominated by carbon as desired. The carbon content obtained in this study is also similar to the previously reported carbon content with different carbon materials, such as from durian [19] and palm date [20].

Table 1. The chemical content for AC-2.0 and AC-2.5 samples

Contents	AC-2.0		AC-2.5	
	Mass %	Atom %	Mass %	Atom %
C	87.99	92.01	91.7	94.62
O	8.24	6.47	5.5	4.26
Mg	1.19	0.61	0.98	0.5
Si	0.53	0.24	0.24	0.1
P	0.23	0.09	0.19	0.08
K	0.91	0.29	0.65	0.21
Ca	0.92	0.29	0.73	0.23
Totals	100%	100%	100%	100%

In addition to carbon, the oxygen element also dominates the sample. The presence of oxygen elements is obtained from the CO_2 gas at activation process. The oxygen element has the second highest percentage after Carbon element, the cause is indicated by the carbonization of oxygen in the carbon samples which do not decompose completely or the bond occurs in the activation process. Carbon element quantity in AC-2.5 sample is greater than AC-2.0 sample. Increasing activation time will cause the quantity of content other than carbon to decompose more, so that the carbon element produced be higher.

3.4. X-ray diffraction (XRD) Analysis

X-ray diffraction is a method to determine whether a material is amorphous or crystalline. The XRD pattern of carbon samples derived from pineapple crown biomass with a activation time variation of 2 hours and 2.5 hours is shown in Figure 3. Characterization show that there are two broadening peaks with a diffraction angle (2θ) in range of 10˚ to 100˚. Determination of diffraction angle for each peak was done by using Microcal Origin software. Data is fitted by the lorentzian distribution function. From the fitting data obtained the diffraction angle, peak height and peak width. The AC-2.0 sample has two broadening peaks at a 2θ angle of 25.108˚ and 44.214˚ and it are correspond to the scattering plane (002) and (100). While the AC-2.5 sample has a 2θ angle of 24,749˚ and 43,768˚.

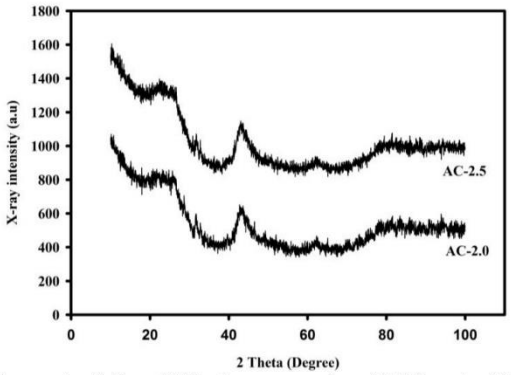

Figure 2. X-Ray Diffraction curve for AC-2.0 and AC-2.5 samples

Table 2 shows that the 2θ angle undergo a shift for samples that were activated at 2 and 2.5 hours. The 2.5 hour activation time has a 2θ angle (002) and (100) close to a universal peak which is 24˚ and 44˚ for carbon peak compared to a 2 hour activation time. This analysis is indicated because a 2.5 hour sample has a higher carbon purity compared to a 2 hour activation time such as EDX data which it discussed earlier. The microcrystalline height data (L_c) shows the existence reguler value based on the activation time variation. The L_c on the AC-2.0 sample is greater than the L_c for the AC-2.5 sample. The relationship of the microcrystalline height (L_c) of graphite in the carbon electrode to the specific surface area is given by the empirical formula $SSA_{xrd} = 2/(\rho_{xrd} L_c)$, where ρ_{xrd} = X-ray density given with the formula $\rho_{xrd} = \{d_{002\ (graphite)} / d_{002}\}\rho_{(graphite)}$ [21, 22]. Based on the empirical formula, to produce a higher surface area of carbon electrodes, a smaller interlayer spacing (d_{002}) and microcrystalline height (L_c) are needed. Based on the equation previously, specific surface area obtained for 2 hours sample was 1484.67 $m^2\ g^{-1}$ and specific surface area for AC-2.5 hours was 1856.54 $m^2\ g^{-1}$. This specific surface area are similar as the electrode surface area of other materials, such as cococnut husk and cassava peel waste, which are 28982 $m^2\ g^{-1}$ [7] and 1352 $m^2\ g^{-1}$ [23], respectively. The microcrystalline width (L_a) data shows a significant difference in the variation of activation time in each sample. The AC-2.0 activation time shows a L_a of 25.5839 Å while the AC-2.5 sample has a L_a of 39.8201 Å, where the longer the activation time is the greater L_a. Based on this data it can be concluded that the La is influenced by the length of time of sample activation.

Table 2. Diffraction angle (2θ), interlayer spacing (d), microcrystallinity height (L_c) and microcrystallinity width (L_a) for AC-2.0 and AC-2.5 samples

Sample codes	$2\theta_{(002)}$ (˚)	$2\theta_{(100)}$ (˚)	$d_{(002)}$ (Å)	$d_{(100)}$ (Å)	L_c (Å)	L_a (Å)
AC-2.0	25.108	44.214	3.544	2.047	14.195	25.584
AC-2.5	24.749	43.768	3.594	2.067	13.689	39.820

3.5. Electrochemical Properties Analysis

The electrochemical Measurement of supercapacitor cells was carried out using the Cyclic Voltammetry (CV) method based on two electrode systems in 1M H_2SO_4 electrolyte. Figure 4 is a voltammogram data that shows the relationship between C_{sp} (Fg^{-1}) to voltage (V). The scan rate given is 1 mV s^{-1} at a voltage of 0 to 0.5 V [24]. The selection of the scanning rate of 1 mV s^{-1} is based on the assumption that ion diffusion is more evenly distributed throughout the surface and pores of

carbon electrodes so that the ion pair formation be more perfect, which eventually results in greater specific capacitance [25].

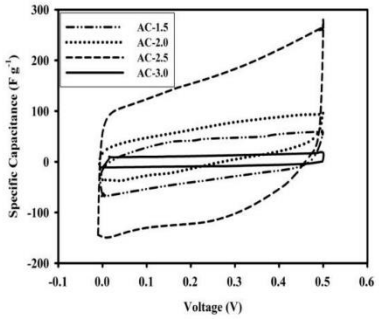

Figure 4. CV curve for all samples

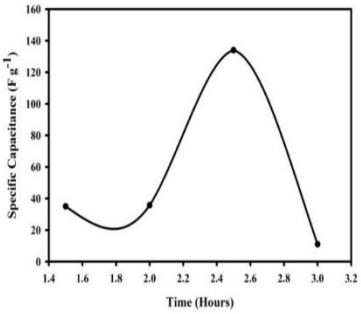

Figure 5. Correlation Specific capacitance with activation time

All samples have specific capacities of 35 Fg^{-1}, 36 Fg^{-1}, 134 Fg^{-1} and 10 Fg^{-1} for samples of AC-1.5, AC-2.0, AC-2.5 and AC-3.0, respectively. The AC-2.5 sample is the sample with the highest specific capacitance, while the AC-3.0 sample is the sample that has the smallest specific capacitance. The maximum specific capacities produced in this study are almost the same as the specific capacitance with different biomass materials that have been studied, such as rubber wood sawdust with specific capacitance of 150 Fg^{-1} [26] and cow dung with specific capacitance of 124 Fg^{-1} [27]. The difference in the specific capacitance is strongly influenced by the density of the activated carbon electrode. Density is inversely proportional to porosity, it mean that the greater the density of the sample, the porosity will be smaller. Porosity is directly proportional to the surface area, the greater the porosity of the sample, the greater the surface area. High surface area gives the opportunity for more ions to experience diffusion resulting in maximum capacitive properties. Measurements obtained of the AC-2.5 sample has the smallest density and the largest specific capacitance value, while the AC-3.0 sample has the largest density and the smallest specific capacitance. Specific capacitance is also influenced by the addition activation time which be seen in Figure 5. In the figure 5, it can be seen that the longer the activation time will be increase the specific capacitance, but when the 3 hour activation time will decrease in the specific capacitance. The 2.5 hour is the activation time with the highest specific capacitance, this is because at that time the meso and micro pores formed are very good. The combination of micro pore and meso pore which more than 2.5 hours develops into larger pores and became macro pores. The decreasing of specific capacitance for AC-3.0 is indicated the 3 hour activation time caused enlargement the micro and meso pore into macro pores.

4. Conclusion

The production of activated carbon electrodes from pineapple crown waste based on variation of activation time for supercapacitor device has been succesfully done. The optimum activation time was found at 2.5 hours which shown by the good physical and electrochemical properties. The good physical properties inclued of lowest density, fiber structure of surface morfology, highest carbon content and larger specific surface area. This good physical properties supports to found an excelent electrochemical properties with the highest spesific capacitance as high as 134 F g^{-1}.

Acknowledgements

1. We would like to thank the Rector of the Islamic State University of Sultan Syarif Kasim Riau for the finansial support by using the basic cluster of scientific integration 2018 with the Principal

researcher of Dr. Rika, S.Si., M.Sc with the project titled "Utilization of aquatic weed plants as the raw material for the production of supercapacitor electrodes" with contract number: 0935/R/2018.

2. The author also would like to thank the DRPM Kemenristek-Dikti through the second year Project of PDUPT with the title "Potential of Urban Solid Waste Utilization as a Supercapacitor Electrode" with contract number: 360/UN.19.5.1.3/PP/2018. The author also thanks the SEM FMIPA ITB Laboratory, which has assisted in obtaining the SEM and EDX data.

References

[1] Itagaki M, Suzuki S, Shitanda I, Watanabe K, Nakazawa H 2007 *J. Power Sources* **164** 415
[2] Borenstein A, Hanna O, Attias R, Luski S, Brousse T, Aurbach D 2017 *J. Mater. Chem.* **5** 12653
[3] Sun X, Sun H, Li H, Peng H 2013 *Adv. Mater.* **25** 5153
[4] Noked M, Okashy S, Zimrin T, Aurbach D 2012 *Angew. Chem., Int. Ed.***51** 1568
[5] Deraman M, Saad S K M, Ishak M M, Awitdrus,Taer E, Talib I, Omar R, Jumali M H H 2014 the third nanoscale and nanotechnology sympsium. Malaysia
[6] Chaitra K, Vinny R T, Sivaraman P N, Reddy K,Venkatesh, Nagaraju N, Kathyayini N, Vivek C S 2017 *J. Energy Chem.* **26** 56
[7] Yin L, Chen Y, Li D, Zhao X, Hou B, Cao B 2016 *Mater. Design* **111** 44
[8] Abioye A M, Ani F N 2015 *Renewable and Sustainable Energy Reviews* **52** 1282
[9] Taer E, Taslim R, Mustika W S, Kurniasih B, Agustino, Afrianda A, Apriwandi 2018 *Int. J. Electrochem. Sci.* **13** 8428
[10] N. S. M. Nor, M. Deraman, R. Omar, E. Taer, Awitdrus, R. Farma, N. H. Basri, and B. N. M. Dolah, AIP Conf. Proc. 1586, 68-73 (2014); doi: 10.1063/1.4866732
[11] Efi Respati, Outlook komoditas pertanian Nenas. 2016. Pusat Data dan Sistem Informasi Pertanian Sekretariat Jenderal Kementerian Pertanian, jakarta. Indonesia
[12] Taer E and Taslim R 2018 *AIP Conf. Proc.* **1927** 020004-1
[13] Taer E, Deraman M, Talib I A, Awitdrus A, Hashmi S A and Umar A A 2011 *Int. J. Electrochem. Sci.* **6** 3301
[14] Taer E, Apriwandi, Yusriwandi, Mustika W S, Zulkifli, Taslim R, Sugianto, Kurniasih B, Agustino and Dewi P 2018 *AIP Conf. Proc.* **1927** 030036-1
[15] Taer E, Deraman M, Taslim R, Iwantono 2013 *AIP Conf. Proc.* **1554** 33
[16] González A, Goikolea E, Barrena J A, Mysyk R 2016 *Renewable and Sustainable Energy Reviews* **58** 1189
[17] Taer E, Sugianto, Sumantre M A, Taslim R, Iwantono, Dahlan D and Deraman M 2014 *Adv. Mat. Research* **896** 66
[18] Iwantono, Taer E, Umar A A 2012 *AIP Conf. Proc.* **1454** 251
[19] Taer E, Dewi P, Sugianto, Syech R, Taslim R, Salomo, Susanti Y, Purnama A, Apriwandi, Agustino, Setiadi R N 2018 *AIP Conf. Proc.* **1927** 030026-1
[20] Shoaib M, Al-Swaidan H M 2015 *Biomass and bioenergy,* **73** 124
[21] Deraman M, Daik R, Soltaninejad S, Nor N S M, Awitdrus, Farma R, Mamat N F, Basri N H, Othman M A R 2015 *Adv. Mater. Research* **1108** 1
[22] Kumar K, Saxena R K, Kothari R D, Suri K, Kaushik N K, Bohra J N 1997 *Carbon* **35** 1842
[23] Ismanto A E, Wang S, Soetaredjo F E, Ismadji S 2010 *Bioresource Technol.* **101** 3534
[24] Inagaki M, Konno H, Tanaike O 2010 *J. Power Sources* **195** 7880
[25] Taer E, Zulkifli, Sugianto, Taslim R 2015 *Prosiding Seminar Nasional Fisika* 05
[26] Farma R, Deraman M, Awitdrus A, Talib I A, Taer E, Manjunatha J G, Ishak M M, Dollah B M N, Hashmi S A, Basri N H 2013 *Bioresource Technol.* **132** 254
[27] Bhattacharjya D, Yu J-S 2014 *J. Power Sources* **262** 224

Advanced Studies in Theoretical Physics
Vol. 12, 2018, no. 6, 257 - 265
HIKARI Ltd, www.m-hikari.com
https://doi.org/10.12988/astp.2018.8625

Conductive-Convective Heat Transfer in an Inclined Enclosure with Vertical Partition

Marhama Jelita

Department of Electrical Engineering
Faculty of Science Technology
State Islamic University of Sultan Syarif Kasim
28293 Pekanbaru, Riau, Indonesia

Rika Taslim

Department of Industrial Engineering
Faculty of Science Technology
State Islamic University of Sultan Syarif Kasim
28293 Pekanbaru, Riau, Indonesia

Abstract

Conductive–convective heat transfer in a square enclosure are studied numerically in the present article. The hot and cold walls are making an angle with horizontal direction. The Galerkin weighted residual finite element method has been used to solve the governing partial differential equations. In numerical simulations, the partition thickness, the orientation angle and the Rayleigh number are considered. It is found that the flow circulation decreases with decreasing the orientation angle and the maximum heat transfer rate is obtained near $\varphi = 60°$ for the considered partition thickness.

Keywords: conjugate convection, finite element method, comsol

1 Introduction

Thermally driven flow and heat transfer in a differentially heated enclosures from side or below has received considerable attention over the past few decades, largely due to a wide variety of applications, which include building technology, electronic boxes, solar collector technology, energy storage, nuclear reactor technology, etc. Comprehensive theoretically or experimentally studies have been conducted by many authors. The topic of these studies is mostly enclosure bounded or partitioned by solid walls with zero thickness. In some situations, the conductivities of the enclosure walls and the fluid inside are comparable and the wall thickness is finite, for example in the high performance insulation for buildings. This coupled conduction-convection problem is called as conjugate convection. [1] studied a rectangular enclosure with a vertical partition and filled with air. They found that partitioning is an effective method of reducing heat transfer and the maximum reduction in heat transfer occurs when the partition was placed midway between the vertical walls. The heat transfer rate was found considerably attenuated in a partitioned enclosure in comparing with that for non-partitioned enclosure as reported by [2]. [3] studied numerically and experimentally enclosures with multiple vertical partitions and showed that the Nusselt number is inversely proportional to the number of partitions. [4] investigated the conductive multiple partitions and side walls and found the mean Nusselt number decreases with increasing of partition number. [5] compared the numerical and experimental results for a cubic enclosure without and with a partition. They concluded that the introduction of a complete vertical partition reduces convective heat transfer from 59.1% to 63.6% in the range of Rayleigh numbers $38,000 < Ra < 369,000$. [6] reported the average Nusselt number increases with decreasing of thermal resistance of the partition and the partition thickness has little effect on heat transfer. [7] studied a vertically divided square enclosure by a solid partition into air and water regions and found that filling of fluid into chests is important for obtaining maximum heat transfer and energy saving. [8] addressed on the optimization of heat transfer rate by varying the partitions location, partitions size and thermal conductivity ratio. Recently, [9] concluded that the partition position has a negligible effect on the average Nusselt number.

To the best of our knowledge, no report has been obtained for conductive–convective heat transfer in an inclined square enclosures partitioned by conductive wall. Controlling the heat transfer using a partition and varying the orientation angle are essential in industrial applications or in a building construction. The aim of this work is to solve numerically the conductive-convective heat transfer in an enclosure with vertical partition. The hot and cold walls are making an angle with horizontal direction.

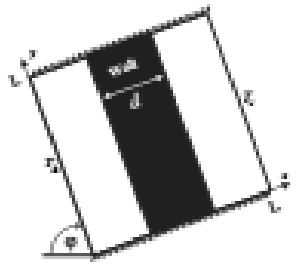

Figure 1: Schematic representation of the model.

2 Mathematical Formulation and Solution

A schematic diagram of an inclined square enclosures with sides of length L is shown in Figure 1. The hot wall is making an angle of φ with horizontal direction. For $\varphi = 0°$, hot wall becomes the bottom wall whereas for $\varphi = 90°$, it becomes the left vertical wall. Opposite to the hot wall is the cold wall. Other two walls are maintained at adiabatic condition. Thermophysical properties of the fluid in the flow field are assumed to be constant except the density variations causing a body force term in the momentum equation. The Boussinesq approximation is invoked for the fluid properties to relate density changes to temperature changes, and to couple in this way the temperature field to the flow field. Under the above assumptions, the governing equations for steady natural convection flow using conservation of mass, momentum and energy can be written as

$$\frac{\partial u}{\partial x} + \frac{\partial v}{\partial y} = 0 \tag{1}$$

$$u\frac{\partial u}{\partial x}+v\frac{\partial u}{\partial y}=-\frac{1}{\rho}\frac{\partial p}{\partial x}+\nu\left(\frac{\partial^2 u}{\partial x^2}+\frac{\partial^2 u}{\partial y^2}\right)$$
$$-g\beta\left(T_f-T_c\right)\cos\varphi \tag{2}$$
$$u\frac{\partial v}{\partial x}+v\frac{\partial v}{\partial y}=-\frac{1}{\rho}\frac{\partial p}{\partial y}+\nu\left(\frac{\partial^2 v}{\partial x^2}+\frac{\partial^2 v}{\partial y^2}\right)$$
$$+g\beta\left(T_f-T_c\right)\sin\varphi \tag{3}$$
$$u\frac{\partial T_f}{\partial x}+v\frac{\partial T_f}{\partial y}=\alpha\left(\frac{\partial^2 T_f}{\partial x^2}+\frac{\partial^2 T_f}{\partial y^2}\right) \tag{4}$$

and the energy equation for the solid divider are:

$$\frac{\partial^2 T_w}{\partial x^2}+\frac{\partial^2 T_w}{\partial y^2}=0 \tag{5}$$

where the subscripts f and w stand for the fluid and the wall respectively. No-slip condition is assumed at all the solid-fluid interfaces. The values of the velocity are zero in the solid regions and on the solid-fluid interfaces. Continuity of the heat flux at the solid-fluid interfaces in both enclosures

$$\frac{\partial T_f}{\partial y}=K_r\frac{\partial T_w}{\partial y} \tag{6}$$

where $K_r=k_w/k_f$ is the thermal conductivity ratio. At the same time, continuity of the temperature at the solid-fluid interfaces is represented by $T_f=T_w$.

The governing equations with the boundary conditions are solved numerically by employing Galerkin weighted residual finite element method. The basic idea of this method is dividing the whole domain into smaller elements of finite dimensions called finite elements. The solution domain is generated into finite element meshes, which are composed of non-uniform triangular elements. The triangular mesh distribution calibrates for fluid dynamics condition. We consider the Laminar Flow (spf) for the continuity and momentum equation and Heat Transfer (Ht) for the convection and conduction equations. Figure 2 shows the snapshot of the Comsol program illustrating the triangular mesh distribution with an extra fine element size and the model builder settings.

After the convergence is reach then the Nusselt number or the heat transfer are calculated. We present the flow circulation using the streamfunction which is derived from the first derivative of velocities.

3 Results and Discussion

The analysis in the undergoing numerical investigation are performed in the following range of the associated dimensionless groups: the partition thickness, $0.0 \leq D \leq 1.0$, the inclination angle of the enclosure, $0^\circ \leq \varphi \leq 90^\circ$ and the

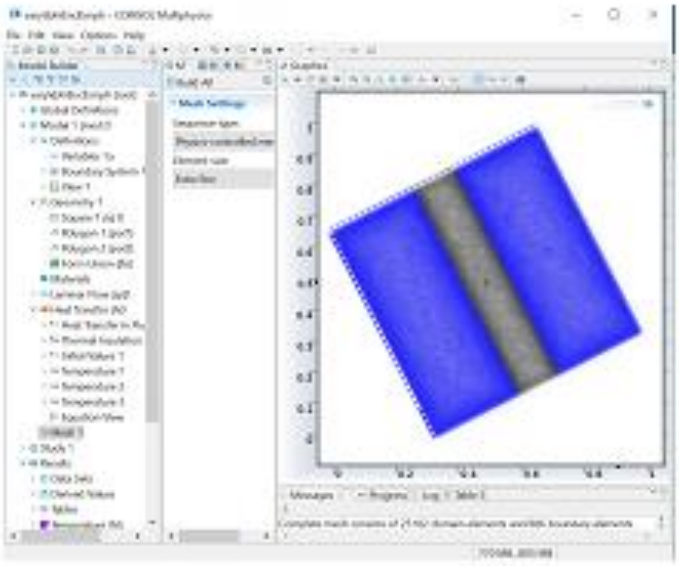

Figure 2: Snapshot of the Comsol program.

Rayleigh number $10^3 \leq Ra \leq 10^6$. The Prandtl number is fixed at $Pr = 0.71$ and $K_r = 1$. The flow and temperature fields are presented in terms of streamline and isotherms contours, respectively. The heat transfer rate is represented by the average Nusselt number.

Figure 3 shows the streamlines and isotherms to show the effects of inclination angle on flow fields and thermal distribution for $D = 0.2$. Some of heat released by the hot surface and travels with the fluid in the hot portion, the partition wall released the heat again to fluid in the cold portion and it terminates at the cold surface. These create rotating cells circulation. Flow strength measured by the level labels. The flow circulation decreases with decreasing the orientation angle. The monocellular flow in the hot portion are negative dilation of the monocellular flow in the cold portion. The core vortex of the hot partition occurs at lower part while the core vortex of the cold partition occurs at upper part. For all angles, the isotherms in the solid partition are almost parallel with hot and cold surfaces. This is an evident that the partition acts as a thermal barrier.

Variations of the average Nusselt number is shown Fig. 4 for different values of Ra with constant values of $D = 0.2$. Obviously, the average Nusselt number is increased as the Rayleigh number increases for any orientation angle. The average Nusselt number profile exhibit parabolic curve for the both cases except at the $Ra = 10^3$. This due to at $Ra = 10^3$, the both morphology stay in the conduction heat transfer mode at any orientation angle. At $Ra = 10^4$, The average Nusselt number remains 1, indicating almost no convection occur inside the enclosure. For higher buoyancy force, the partition wall blocks the convective flow at $\varphi = 0°$ or Bénard convection problem. Later, the partition conducts heat intensively from the hot fluid at higher gravitational force or higher temperature difference. The maximum heat transfer rate is obtained near $\varphi = 60°$.

4 Conclusions

In the present numerical simulations, we have studied the partitioned enclosure with different orientation. The governing equations are solved numerically using the built-in finite element method of COMSOL. Detailed computational results for flow and temperature fields and the heat transfer rate have been presented in the graphical forms. The inclination angle and Rayleigh number affected the shape of streamlines cells, isotherms lines and Nusselt number profiles. We found that the flow circulation decreases with decreasing the orientation angle and the maximum heat transfer rate is obtained near $\varphi = 60°$.

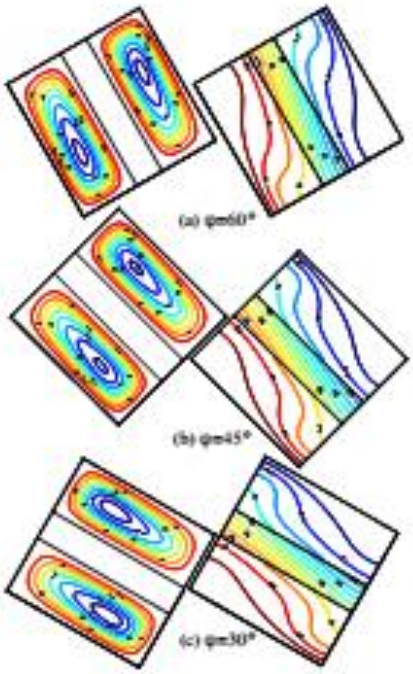

Figure 3: Streamlines (left) and isotherms (right) evolutions for several inclination angles at $D = 0.2$ and $Ra = 10^5$.

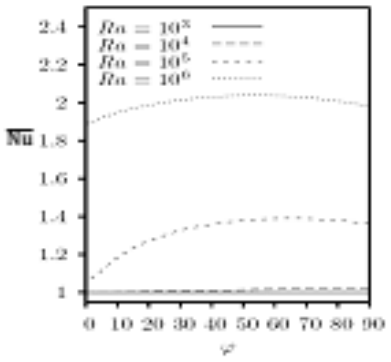

Figure 4: Variation of average Nusselt number with φ for different Ra at $D = 0.2$.

References

[1] T.W. Tong and F.M. Gerner, Natural convection in partitioned air-filled rectangular enclosures, *Int. Comm. Heat Mass Transf.*, **13** (1986), 99–108. https://doi.org/10.1016/0735-1933(86)90076-x

[2] C.J. Ho and Y.L. Yih , Conjugate natural heat transfer in an air-filled rectangular cavity, *Int. Comm. Heat Mass Transf.*, **14** (1987), 91-100. https://doi.org/10.1016/0735-1933(87)90011-x

[3] T. Nishimura, M. Shiraishi, F. Nagasawa and Y. Kawamura, Natural convection heat transfer in enclosures with multiple vertical partitions, *Int. J. Heat Mass Transf.*, **31** (1988), 1679-1686. https://doi.org/10.1016/0017-9310(88)90280-3

[4] H. Turkoglu and N. Yucel, Natural convection heat transfer in enclosures with conducting multiple partitions and side walls, *Heat Mass Transf.*, **32** (1996), 1-8. https://doi.org/10.1007/s002310050084

[5] D.M.C. Dzodzo, M.B. Dzodzo and M.D. Pavlovic, Laminar natural convection in a fully partitioned enclosure containing fluid with nonlinear thermophysical properties, *Int. J. Heat Mass Transf.*, **20** (1999), 614-623. https://doi.org/10.1016/s0142-727x(99)00053-3

[6] K. Kahveci, A differential quadrature solution of natural convection in an enclosure with a partial partition, *Numer. Heat Transf. Part A*, **52** (2007), 1009-1026. https://doi.org/10.1080/10407780701364536

[7] H. F. Oztop, Y. Varol and A. Koca, Natural convection in a vertically divided square enclosure by a solid partition into air and water regions, *Int. J. Heat Mass Transf.*, **52** (2009), 5909–5921. https://doi.org/10.1016/j.ijheatmasstransfer.2009.07.016

[8] D.D. Zhang, J.H. Zhang, D. Liu, F.Y. Zhao and H.Q. Wang, Conjugate thermal transport enhancement for an air filled enclosure with heat conducting partitions using inverse convection methodology, *Int. J. Heat Mass Transf.*, **102** (2016), 788–800. https://doi.org/10.1016/j.ijheatmasstransfer.2016.06.030

[9] Mehdi Khatamifar, Wenxian Lin, S.W. Armfield, David Holmes and M.P. Kirkpatrick, Conjugate natural convection heat transfer in a partitioned differentially-heated square cavity, *Int. Comm. Heat Mass Transf.*, **81** (2017), 92–103. https://doi.org/10.1016/j.icheatmasstransfer.2016.12.003

Received: June 21, 2018; Published: September 12, 2018

2. Focus Group Discussion (FGD)


FOCUS GROUP DISCUSSION (FGD)
Outline


FOCUS GROUP DISCUSSION (FGD)
NARASUMBER
Dr. Awitdrus, M.Si


FOCUS GROUP DISCUSSION (FGD)


FOCUS GROUP DISCUSSION (FGD)
CONT


FOCUS GROUP DISCUSSION (FGD)


FOCUS GROUP DISCUSSION (FGD)

3. Proses Pembuatan Elektroda Karbon Superkapasitor dari Eceng Gondok

Eceng gondok

Eceng gondok setelah pemotongan dan pengeringan

Serbuk pra-karbon

Karbonisasi dan aktivasi fisika

Karbon aktif dari eceng gondok

Pelet karbon aktif dari eceng gondok

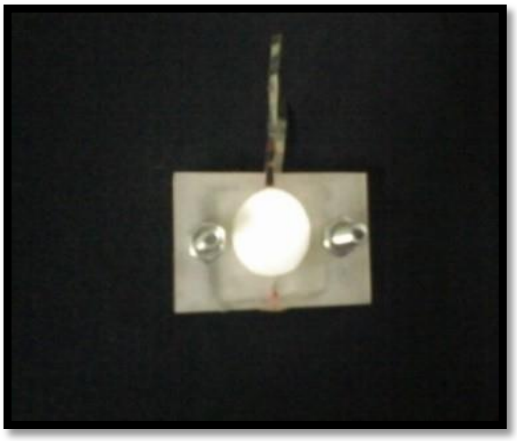

Sel superkapasitor

Pengukuran CV

4. Proses Pembuatan Elektroda Karbon Superkapasitor dari Rumput Purun Tikus

Rumput Purun Tikus

Purun tikus setelah pengeringan dan pemotongan

Serbuk pra-karbonisasi

Aktivasi kimia

Karbonisasi dan aktivasi fisika

Pelet hasil karbonosasi dan aktivasi fisika

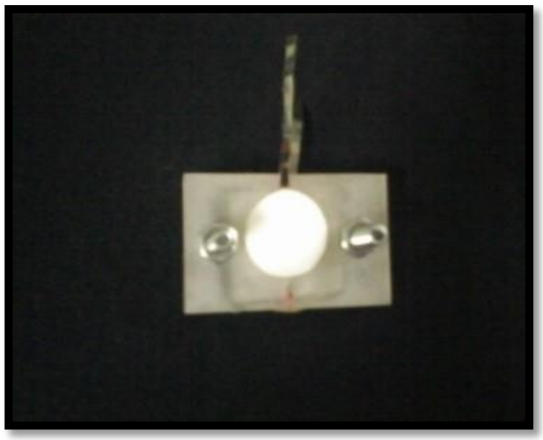

Sel superkapasitor

Pengukuran CV

5. Hasil Pengujian Sifat Fisis dan Elektrokimia Elektroda Karbon Superkapasitor

- Uji TGA

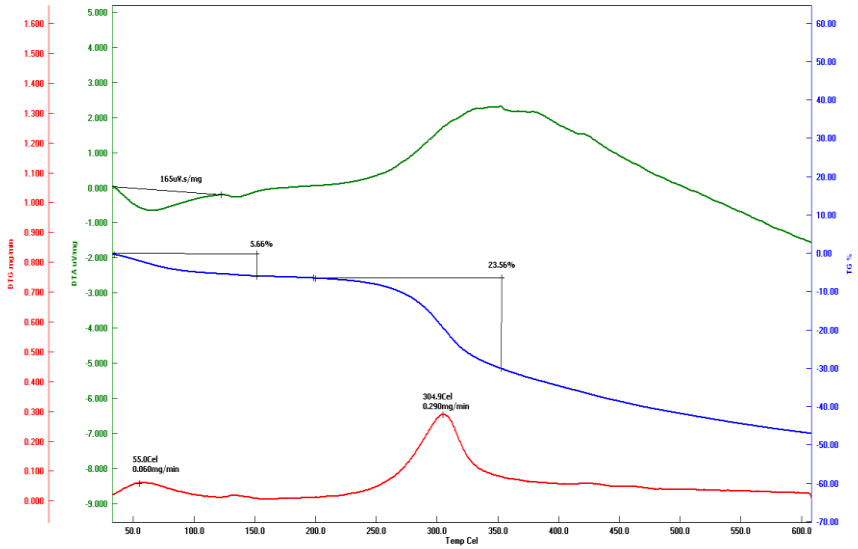

- Hasil Pengujian Morfologi Permukaan menggunakan *Scanning Electron Microscopy* (SEM)

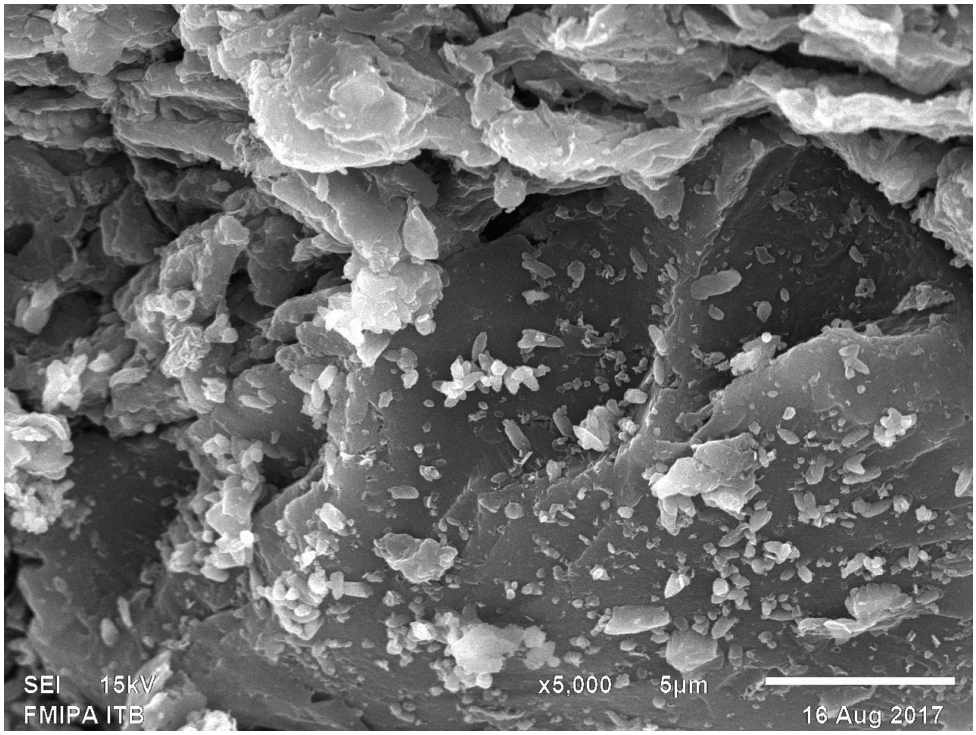

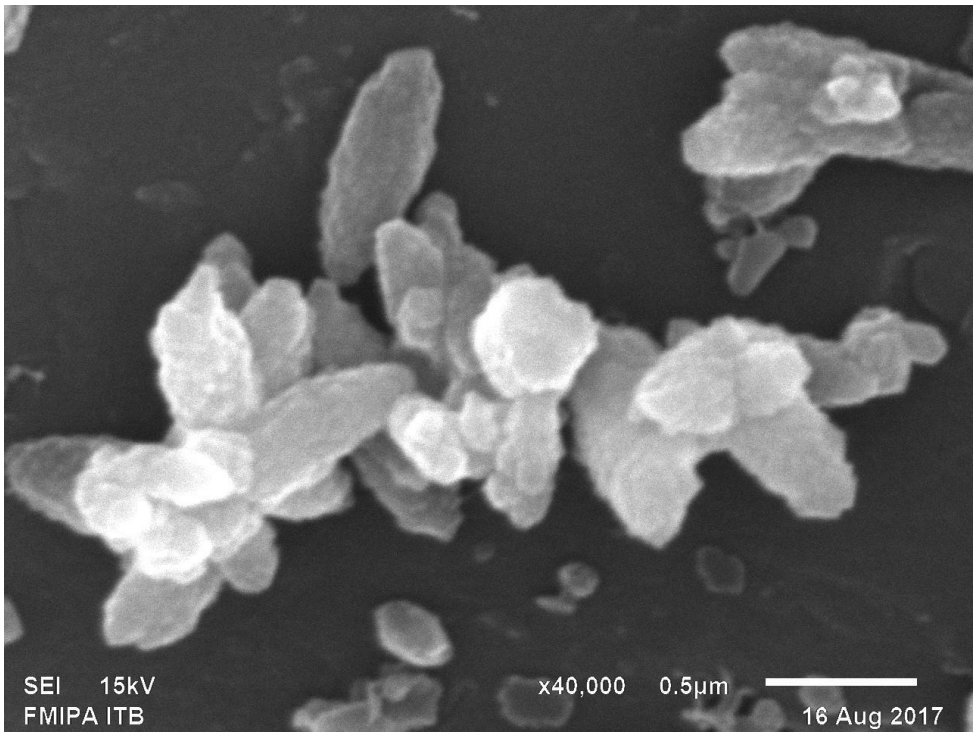

- Hasil Pengujian Energi dispersif sinar-X

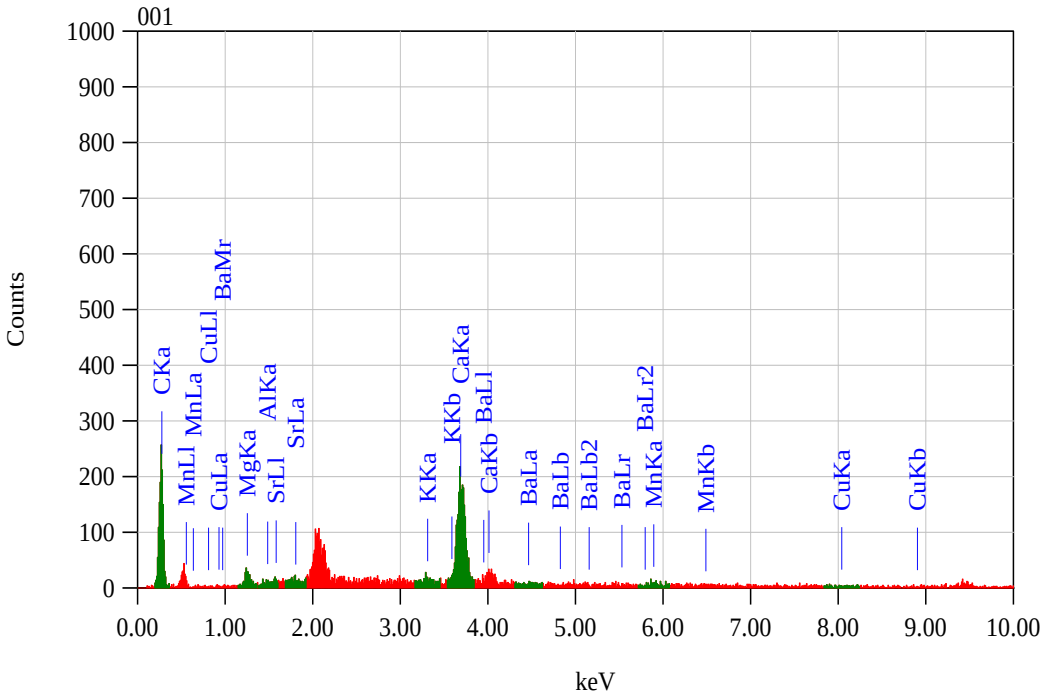

- Hasil Pengujian difraksi sinar-X

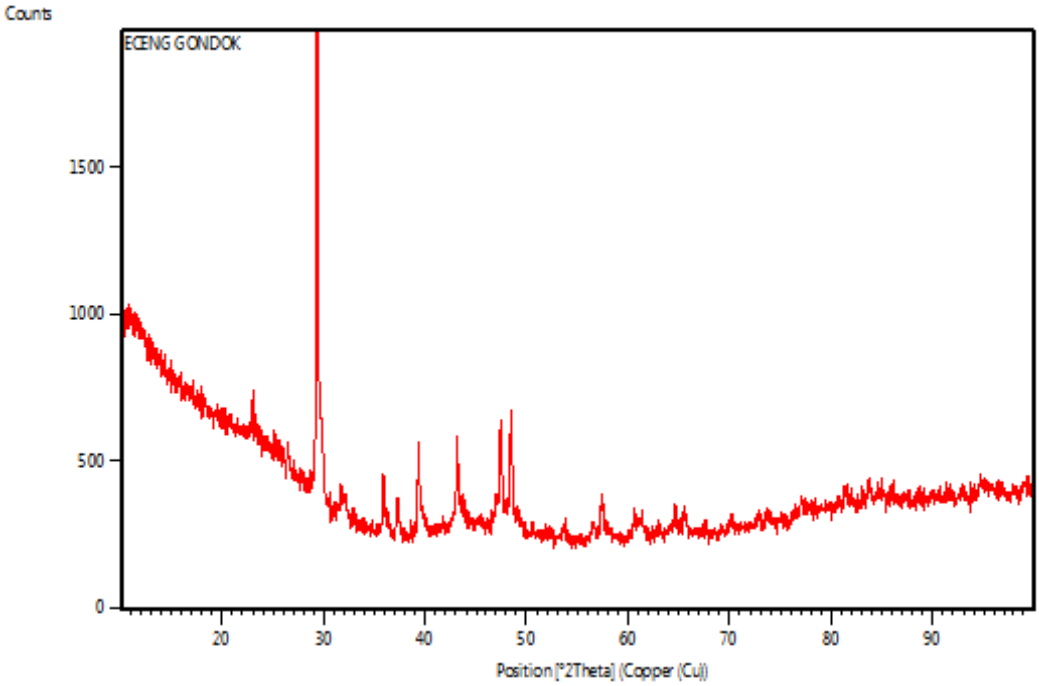

- Hasil Pengujian Serapan Gas N_2

Quantachrome NovaWin - Data Acquisition and Reduction
for NOVA instruments
©1994-2010, Quantachrome Instruments
version 11.0

Quantachrome INSTRUMENTS
Optimizing particle performance

Analysis				Report			
Operator:	nova	**Date:**	2017/10/24	**Operator:**	nova	**Date:**	11/1/2017
Sample ID:	EG	**Filename:**		C:\QCdata\Physisorb\EG.qps			
Sample Desc:		**Comment:**		Agustino			
Sample weight:	0.0358 g	**Sample Volume:**		0.0105 cc	**Sample Density:**		3.41 g/cc
Outgas Time:	3.0 hrs	**OutgasTemp:**		300.0 C			
Analysis gas:	Nitrogen	**Bath Temp:**		77.3 K			
Press. Tolerance:	0.050/0.050 (ads/des)	**Equil time:**		120/120 sec (ads/des)	**Equil timeout:**		240/240 sec (ads/des)
Analysis Time:	547.9 min	**End of run:**		2017/10/24 2:42:27	**Instrument:**		Nova Station B
Cell ID:	91				**F/W version:**		0.00

Multi-Point BET

Data Reduction Parameters Data

Adsorbate	Nitrogen	Temperature	77.350K		
	Molec. Wt.: 28.013 g	**Cross Section:**	16.200 A²	**Liquid Density:**	0.808 g/cc

Multi-Point BET Data

Relative Pressure [P/Po]	Volume @ STP [cc/g]	1 / [W((Po/P) - 1)]	Relative Pressure [P/Po]	Volume @ STP [cc/g]	1 / [W((Po/P) - 1)]
2.68080e-02	158.7657	1.3882e-01	1.75844e-01	217.9947	7.8311e-01
5.31990e-02	173.7127	2.5880e-01	2.14877e-01	228.3009	9.5917e-01
8.48430e-02	187.7062	3.9518e-01	2.38064e-01	234.3746	1.0666e+00
1.20541e-01	201.1168	5.4528e-01	2.69197e-01	242.4868	1.2154e+00
1.55241e-01	212.1567	6.9305e-01	3.09375e-01	252.0139	1.4222e+00

BET summary

Slope =	4.477
Intercept =	1.005e-02
Correlation coefficient, r =	0.999510
C constant=	446.502
Surface Area =	776.213 m²/g

- Hasil Pengukuran menggunakan *Cyclic Voltammetry*